COMPARISON OF METALLURGICAL PROPERTIES FOR INCONNEL 718 PRODUCED ON AN EOS M270 LASER MELTING MACHINE

A THESIS SUBMITTED TO
THE GRADUATE SCHOOL OF NATURAL AND APPLIED SCIENCES OF
KARABUK UNIVERSITY

BY

ABDULLAH SEYIR

IN PARTIAL FULFILLMENT OF THE REQUIREMENTS FOR
THE DEGREE OF MASTER OF SCIENCE IN
DEPARTMENT OF
INDUSTRIAL DESIGN ENGINEERING

September 2019

I certify that in my opinion the thesis submitted by Abdullah SEYIR titled "COMPARISON OF METALLURGICAL PROPERTIES FOR INCONNEL 718 PRODUCED ON AN EOS M270 LASER MELTING MACHINE" is fully adequate in scope and in quality as a thesis for the degree of Master of Science.

Prof. Dr. Mustafa YASAR ....
Thesis Advisor, Department of Industrial Design Engineering

This thesis is accepted by the examining committee with a unanimous vote in the Department of Computer Engineering as a master thesis. September 24, 2019

Examining Committee Members (Institutions)	Signature
Chairman: Prof. Dr. Yahya ALTUNPAK (BAIBU)	....
Member : Prof. Dr. Mustafa YASAR (KBU)	....
Member : Assist. Prof. Dr. Hatice EVLEN (KBU)	....

...../...../2019

The degree of Master of Science by the thesis submitted is approved by the Administrative Board of the Graduate School of Natural and Applied Sciences, Karabük University.

Prof. Dr. Filiz ERSÖZ ....
Head of Graduate School of Natural and Applied Sciences

“This thesis has been completed in collaboration with University of Wolverhampton, UK and University of Karabuk, Turkey under the European Union Erasmus exchange study programme. I declare that all the information within this thesis has been gathered and presented in accordance with academic regulations and ethical principles and I have according to the requirements of these regulations and principles cited all those which do not originate in this work as well.”

Abdullah SEYIR

ABSTRACT

M. Sc. Thesis

COMPARISON OF METALLURGICAL PROPERTIES FOR INCONNEL 718 PRODUCED ON AN EOS M270 LASER MELTING MACHINE

Abdullah SEYIR

Karabuk University
Graduate School of Natural and Applied Sciences
The Department of Industrial Design Engineering

Thesis Advisor:
Prof. Dr. Mustafa YAŞAR
September 2019, 77 pages

In this study, Inconel 718 alloy has been produced in the EOSINT M270 Laser Melting Machine. This work thus aimed to develop scan speed and step over parameters. These parameters are very important for the quality and properties of the resulting product. To achieve a quality result reference from the accepted parameters was taken; various scan speed and step over distance parameters 12 mm x 12 mm x 5 mm cross sectional INCONEL 718 samples were produced. Samples were used, examined and compared with respect to surface quality, balling, spatter and porosity.

Key Words : Direct Metal Laser Sintering, EOSINT M270, Inconel 718, laser powder, scan speed, step over distance, EOS Parameters, porosity.

Science Code : 916.3.029

ÖZET

Yüksek Lisans Tezi

EOSINT M270 (SLM) MAKİNESİNDE ÜRETİLEN INCONEL 718 ALAŞIMININ MEKANİK ÖZELLİKLERİNİN KARŞILAŞTIRILMASI

Abdullah SEYIR

Karabük Üniversitesi
Fen Bilimleri Enstitüsü
Endüstriyel Tasarım Mühendisliği Anabilim Dalı

Tez Danışmanı:
Prof. Dr. Mustafa YAŞAR

Eylül 2019, 77 sayfa

Bu çalışma için EOSINT M270 Lazer Sinterleme Makinesinde Inconel 718 alaşımından numuneler üretildi. Çalışmada tarama hızı ve adim mesafe parametrelerinin geliştirilmesi hedeflendi. Bu parametreler üretilen malzemenin kalitesi ve mekanik özellikleri açısından çok önemlidir. Yeterli bir sonuca ulaşabilmek adına kabul edilmiş Inconel 718 alasımı için belirlenen standart EOS parametreleri ve alternatif parametreler ile 2 mm x 12 mm x 5 mm dikdörtgen kesitli numuneler üretildi. Üretilen numuneler yüzey kalitesi ve yüzey gözenek boşluğu seviyesi açısından karşılaştırıldı.

Anahtar Kelimeler : EOS, EOSINT M270, Lazer Sinterleme, Inconel 718, Yüzey kalitesi, EOS parametreleri, lazer tarama hızı.

Bilim Kodu : 916.3.029

ACKNOWLEDGMENT

I would like to thank to my advisors, Prof. Dr. Mustafa YASAR, Department of Industrial Design Engineering, University of Karabuk, and Prof. Dr. Mark STANFORD, Faculty of Science and Engineering, University of Wolverhampton for their great interest and assistance in preparation of this thesis.

CONTENTS

Page

Page

LIST OF FIGURES

Page

Page

LIST OF TABLES

Page

SYMBOLS AND ABBREVITIONS INDEX

SYMBOLS

µm : Micrometre

F : Fahrenheit

W : Watt

ABBREVITIONS

DMLS : Direct Metal Laser Sintering

RP : Rapid Prototyping

AM : Additive manufacturing

STL : Surface Tessellation Language or Standard Tessellation Language

SLM : Selective Laser Melting

Ed : Energy Density

PL : Laser beam power

Vs : Scanning speed

H : Hatching (step over) distance

IN 718 :Inconel 718

PART 1

INTRODUCTION

When looking at Rapid Prototyping (RP) technologies, the Direct Metal Laser Sintering (DMLS) has a high potential for direct manufacturing of functional prototypes and tools [1]. The primary advantage of this advancement is that the three-dimensional (3D) components can be immediately manufactured using laser energy bonding powdered materials [2,3]. The quality of materials are very significant for the preferred results, thus researchers have studied in the respect Direct Metal Laser Sintering (DMLS) systems, for example. To create bronze components, Klocke et al [4] researched laser sintering a combination of copper and tin powder. Prabhu and Bourell [5] researched the super solid liquid phase laser sintering of bronze pre-alloyed powder for rapid prototyping, and Greulich et al.[6] created a mix containing a combination of steel and bronze powder s for direct laser sintering. Niu and Chang entirely researched DMLS of high-speed steel powders [7–9]. Das et al [10] identified laser sintering as a combination of super alloy nickel and cermet powders to produce turbine blade tips. Alaoui et al [11] studied on WC-Co soft metal powder laser sintering. The Selective Laser Sintering for stainless 314S has been researched by Hauser et al [12]. Das et al [13] have studied on SLS for Laser sintering for the production quality of the parts, DLS was used by Das et al [13] in the production of high-performance parts. The metal base powder mix for tooling was developed by Petzoldt et al [15]. Furthermore, there has been mention of the viability of the method for the production of engineering components using Powder Ti, ceramics and WC – Co on this study [16]. The fundamental principles of operation of laser sintering machines and the bond mechanism of various powder particles have been reported by Bourell et al [17]. Most of the study works published focus on the development of practical components and the investigation of essential elements of the LSM such as microstructural development, sintering machinery, and process parameter influence

[18-20]. The densification mechanism and the linked microstructural features of the laser processed material depend on both powder characteristics and laser processing parameters have been realized [21].

1.1. AIMS AND OBJECTIVES

The key objective of this study is to develop parameters of scan speed and step over distance in the laser melting of Inconel 178 on the EOS M270 Laser Melting Machine.

- Ascertain optimal scan speed and step over distance parameters in the laser melting for Inconel 718.
- Document effect of step over and scan speed parameters on the quality of Inconel 718 samples.
- Evaluate porosity level of the produced samples.
- Compare samples made by developed parameters to samples made using standard EOS parameters.

Investigate the relation between the porosity levels and energy densities applied to the produced samples.

PART 2

LITERATURE REVIEW

2.1. RAPID PROTOTYPING (RP)

Rapid prototyping technologies have great benefits over other processing methods due to the versatility directly from CAD in the production of free and complex shapes. [22]. Figure 2.1 below presents the Data flow in RP. As shown in the figure, firstly, the desired part is designed and modelled considering the machine capacity (i.e. building platform volume) in 3D CAD environment. Then, the prepared CAD file is converted to the "stl" file format that is compatible with the system. During this process, the machine must be setted considering key process parameters such as scan speed, step over distance, laser power also the material powder should be placed into powder section. After finishing the operation, as a last step the produced part should separated from the base plate by wire electrical discharge machine

.

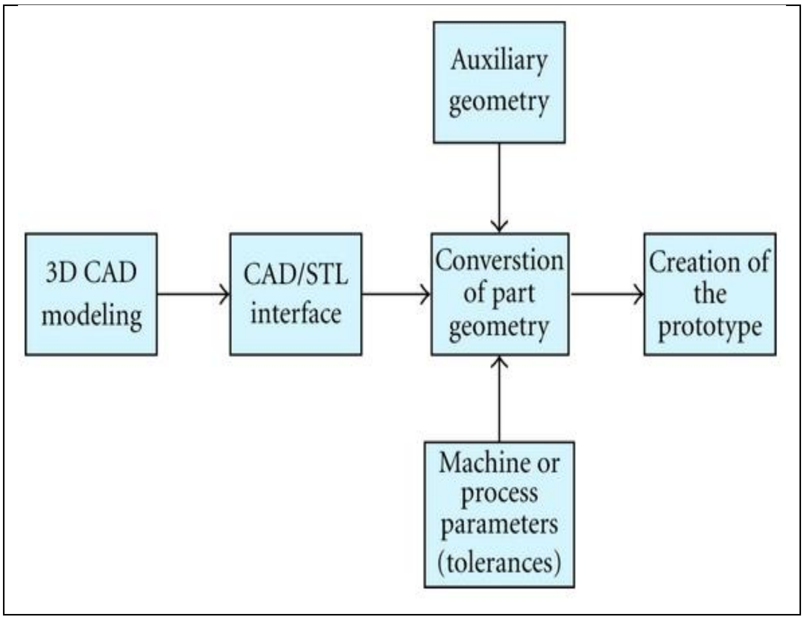

Figure 2.1. Data flow in rapid prototyping [95].

The purpose to use RP (Rapid Prototyping) are shown below:

- Reducing production time,
- Reducing overpriced faults,
- Reducing permanent errors in engineering;
- Extend product life by adding the required functions and removing redundant characteristics early in the design process.

2.2. ADDITIVE MANUFACTURING (AM)

The complex parts can be produced economically with Additive Manufacturing methods compared to traditional manufacturing methods. As well as AM has been developed and started to use for wide range systems in recent ten years [26,27]. Many additive manufacturing methods have been effectively created for metals, varying from aluminium, nickel, metal titanium [29-34].

The same method is applied for each part produced by AM. The solid part created on computer-generated environment (CAD) and it defines the manufacturing of the object through layer [35].

The phases of the method were defined by the addition of materials: modelling for obtaining the 3D model on CAD system [36];

- 3D Model on CAD system.
- Converting to "STL" format for using on CAD system.
- Creating the fixtures;
- Vertical and horizontal manufacturing;
- Preparing the parameters and slicing for production.
- Building the part in machine.
- Removing the fixtures and supports and cleaning of surface.

Following Figure 2.2 describes the different Additive Manufacturing Methods. In this study focused on the powder-based topic.

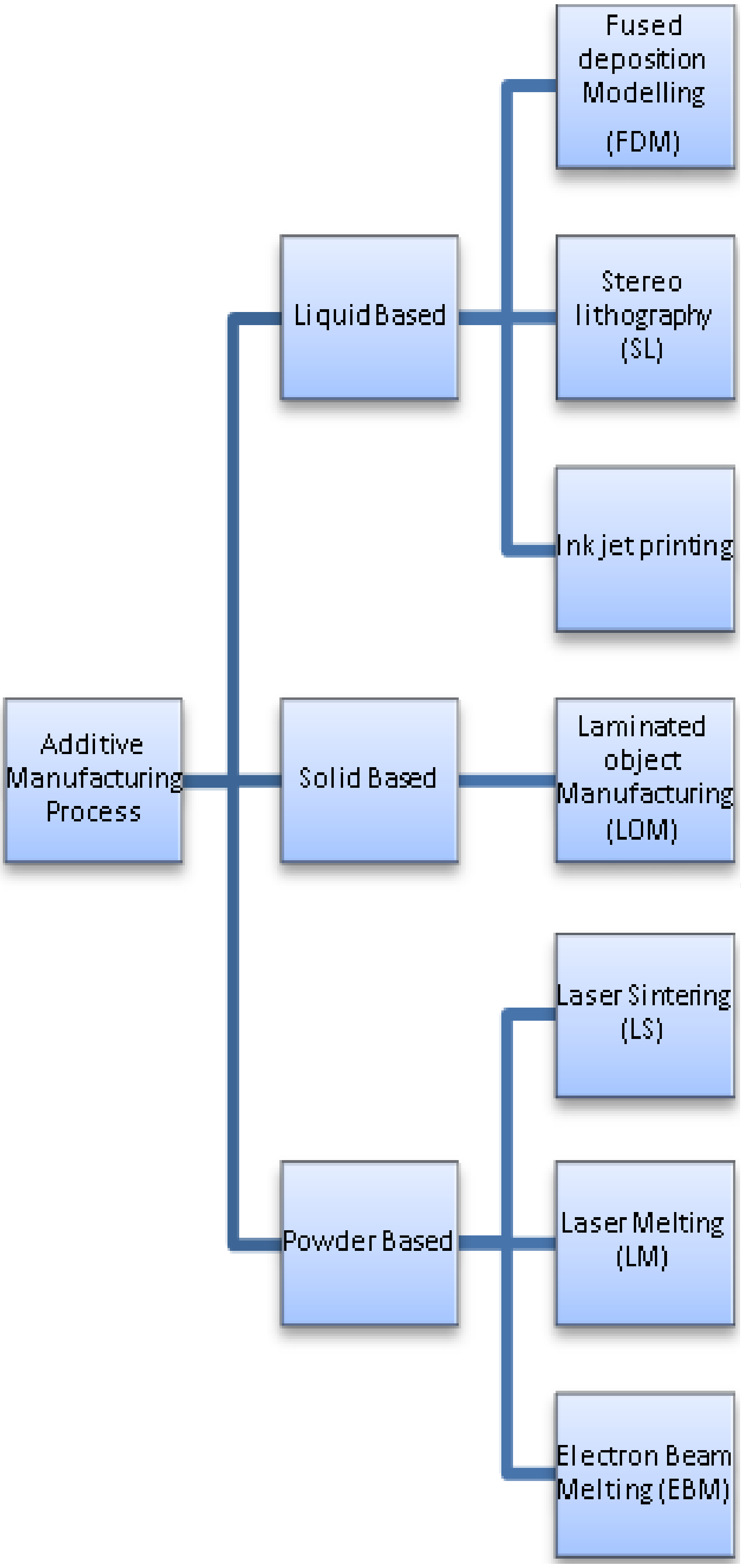

Figure 2.2. Conspectuses of the types additive manufacturing methods [96].

Figure 2.3 below presents the Additive Manufacturing Process with a sample part.The parts are built with layer-by-layer slices. After the creation, the supporting structures must be separated from the main part if they are used in the process.

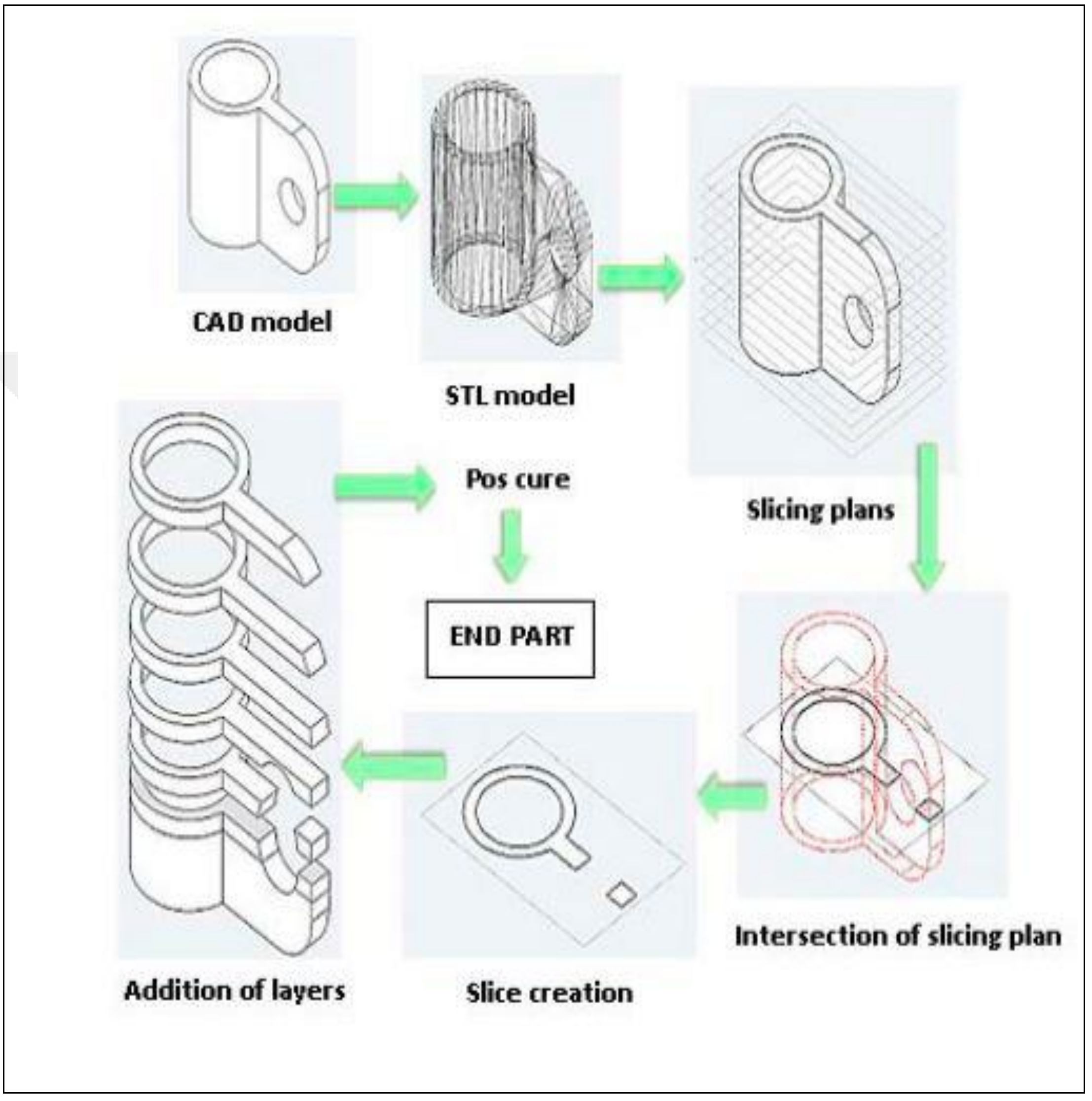

Figure 2.3. Additive manufacturing processes [97].

AM (Additive Manufacturing) allows high speed, adaptable and price-effective manufacturing of components directly from 3D CAD. Therefore, this technology supports development [37].

2.3. SELECTIVE LASER MELTING (SLM)

SLM (Selective Laser Melting) is titled under the Additive Manufacturing system and the 3D parts are manufacturing layer by layer by laser scanning of a powder bed on this method [38]. Manufacturing complex geometries capability is the most important benefit of Selective Laser Melting systems [39]. In addition to Selective Laser Melting system can be used for adapting multi-scale microstructures [40–42]. Selective Laser Melting products have defect-free microstructure due to be out of under the mechanical pressure. The Selective Laser Melting Process bound up with solidification - melting processes and temperature elevation. Those kinds of factors can stimulate irrepressible molten fluids movement and create fault in products which have been built by Selective Laser Melting process. Those faults are reducing to mechanical and fatigue strength [43-45]. Understanding of how faults are created is the key point to reduce such faults.

Figure 2.4 below, shows schematic diagram that represents the general selective laser melting systems. The building cylinder moves towards to -Y direction as one unit per a layer. The powder cylinder provides the required powder for a slice in the opposite direction (+Y) by building cylinder. The recoating device pushes each layer of powder into the section where the part will be created.

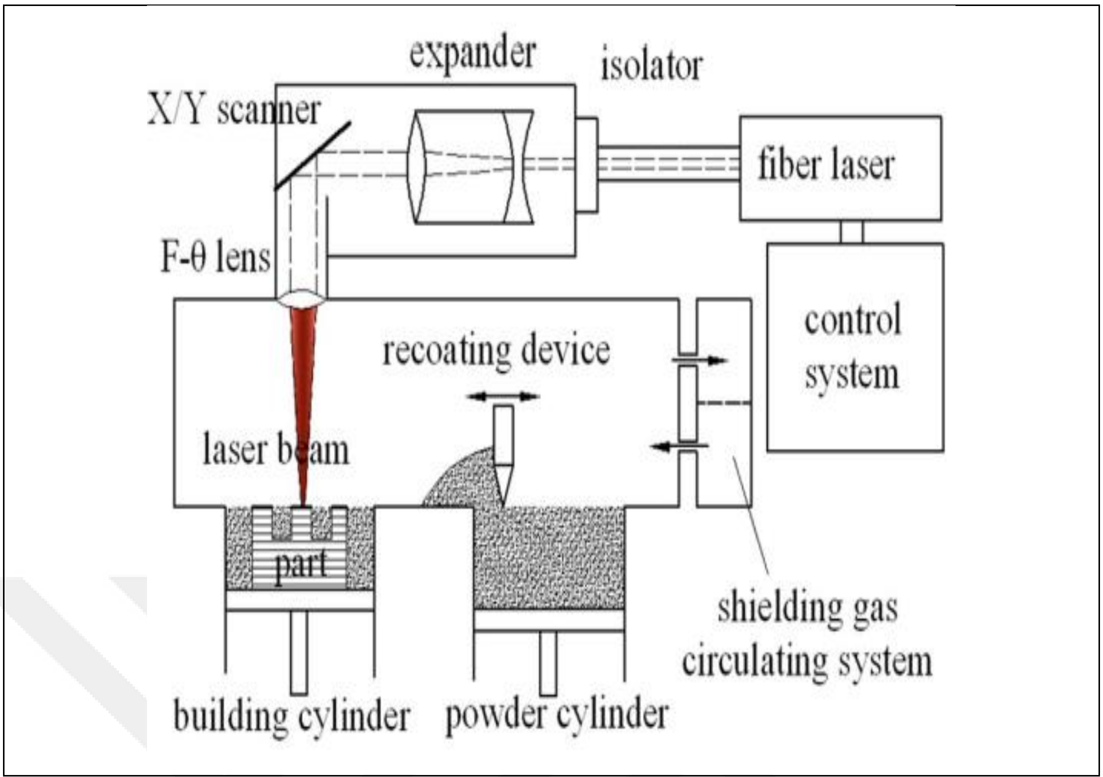

Figure 2.4. Diagram of selective laser melting system [98].

Laser energy applies to selectively melt metal powders layer by layer throughout SLM process and create 3D parts [46,47]. Over complex structured product can be manufacture with this technology [48,49], and due to elimination of material wasting selective laser melting systems are applicable preferable for too many applications. The new material improvement and the effects of processing parameters on microstructure is usually suggested study for Selective Laser Melting systems [50,55]. At the same time selective laser melting is a complicated procedure due to mass transfer and chemical effects [56].

2.4 PROCESSING PARAMETERS OF SLM SYSTEMS

Selective Laser Melting technology is laser base additive manufacturing systems for the produce of metal components [57,60]. Vilaro et al [61] investigated the improvement of pores due to affection of rapid solidification and melting procedure in the Selective Laser Melting procedure. Qiu et al. exanimated pores on the surface of the parts that manufactured by SLM systems and exhibited the reason of the pore could be due to incomplete melting layers. Those studies helped the improvement of porosity. In this study, the splashing material throughout the process of a melting investigated when selective laser melting of aluminium alloy [62-63]. The melt flow dynamic model has been created by Panwisawas et al [64] for the selective laser melting systems in order to clarify the improvement pores under the various circumstances. However, the creation rate of the selective laser melting processes usually low thus the general processes around a 20–30 μm thick powder layer [62-65-66]. In accordance with Ma et al [67] study, the powder layer thickness size variations do not affect the relative density significantly. Figure 2.5 below represents the scanning strategies of selective laser melting systems. (a) standard, (b) diagonal (c) perimeter.

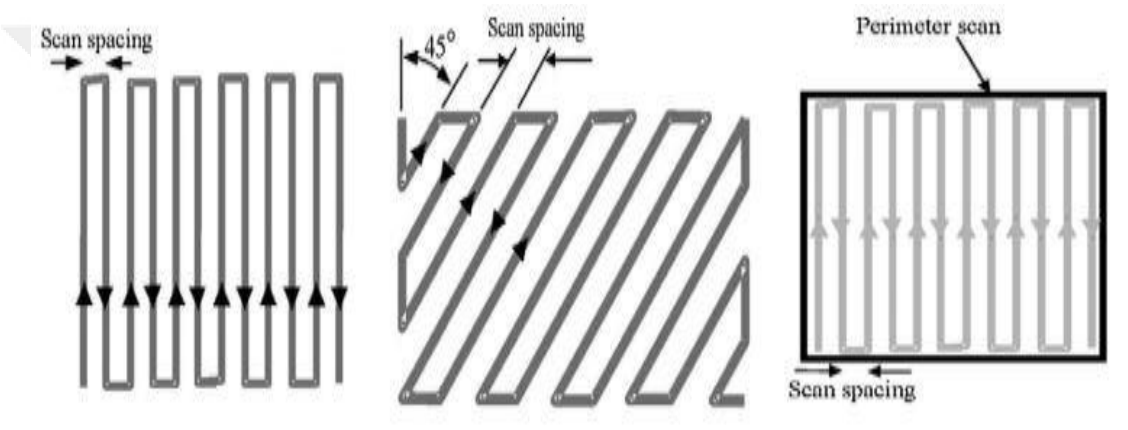

a) b) c)

Figure 2.5. Selective laser systems /selective laser melting scanning strategies [68].

There are various studies to increase the part density. The focus subjects are development of the parameters such as scanning speed, hatch spacing, laser power and layer thickness during the selective laser melting process [68- 71]. At the same time, there are not any study yet considering the changing the strategy for Al alloys. But Thijs et al [72] investigated the impact of scanning processes on the crystallographic texture of the part. Figure 2.6 below shows schematic diagram that represents the general selective laser melting systems. This figure also shows the process parameters.

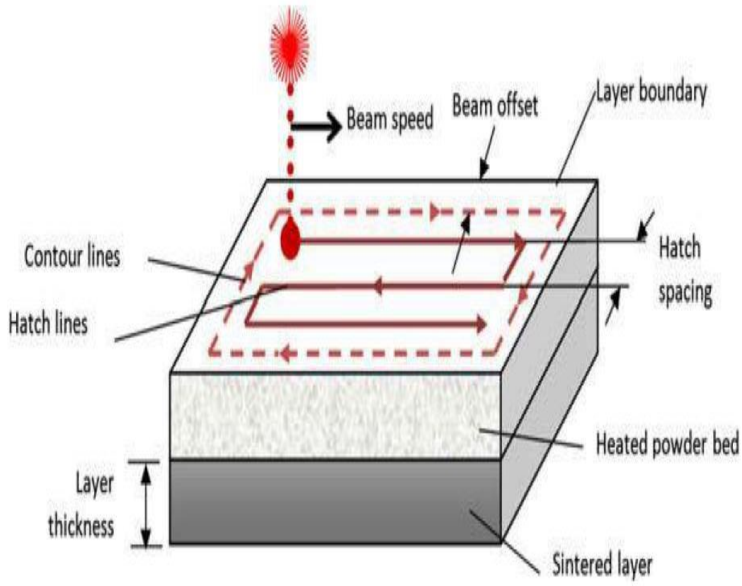

Figure 2.6. SLS/SLM laser and geometry parameters [99].

2.4.1 Laser Power, Scan Speed, Step Over Distance and Layer Thickness

The phenomena related to the laser–powder interaction have been studied by Gusarov and Smurov [73-75]. In this study they calculated the temperature diffusion in to the laser powder effect region and exanimated effect of powder layer thickness and laser scanning speed on the melting form. Dewidar et al [76] explained that local melting could be appearing due to low laser power and scan speed parameters on selective laser systems. According to Khan and Dickens study, [77] to achieve a good consolidation region, laser power range must be between 100 and 240W and the parameter of scan speed must be between 80 mm/s and 200 mm/s.
As well as, parameters of scan speed and laser power are the critical key for the porosity development in the selective laser melting process on ALSi10Mg alloy parts which has been presented by Read et al [78].

The below formula explains the impact of scan speed to the overall energy density in the system reported by Abele et al [79].

$$E_d = P_L / (V_s.H) \tag{2.1}$$

PL = Laser beam power (W), Vs = Scanning speed (mm/s), Ed = Energy Density (J/mm^2), H = Hatching (step over) , Distance (mm).

Thus, modifications or adjustment of the scan speed is obviously effective for the consolidation of the samples, with incidences of roughness, distortion, and irregularities observed due to balling and spatter [80].

Xie et al [81] studied that increased hatch spacing reportedly produced a higher density of laser melted tool steels. Conversely, Khan and Dickens [82] study on the SLM process for gold (Au) concluded that there was not suitable impact on porosity of finished gold samples when the distance of hatch was varied between 80 - 60 and 40μm. In studies by Morgan et al. [83] concluded that unlike scan speed, step over distance has a relatively lower effect on porosity and density of materials.

The layer thickness in laser melting process is a description of how low the piston gets between successive layers. It is thus a parameter that describes powder layer thickness on the powder bed in one cycle for the laser melting process, reported by Gibson et al [84] The literature searching was carried out in accordance with the "aims and objectives" the need of studies related to this subject and has shown its importance. It mentioned all varieties of rapid prototyping technology and especially referred to all stages of Selective Laser Melting system. According to a literature search rapid prototyping systems consists stages of CAD Software, process planning and the manufacturing. In accordance with the literature search the parameters (Layer thickness, Scan Speed and Step Over Distance) which used in the processing of the laser melting systems impact the quality and characteristic properties of the result products. The focus of this study was parameters of Scan Speed and Step over Distance. Under the title of Methodology was presented how to achieve the study aims and all steps of experimental procedure.

PART 3

METHODOLOGY

3.1 EQUIPMENT AND MATERIALS

3.1.1 Inconel 718

In this work, Inconel 718 alloy was produced in the EOSINT M270 Laser Melting Machine. Inconel 718 is a Ni–Cr alloy which has a high-stress rupture, high-strength, and corrosion-resistant. It has the tensile strength of up to 340 MPa with 8% elongation at 870 °C and 1430 MPa with 21% elongation at room temperature [85].

Inconel 718 alloys have excellent processing characteristics, such as hot-workability, good weldability and castability [86]. Due to the properties of good tensile, fatigue, creep, rupture strength and economic manufacturing, Inconel 718 used in a wide range of systems [87]. For these reasonsSuper alloy Inconel 718 is usually used in aerospace/aircraft, petrochemical, and especially nuclear industries [88,89]. Table 3.1 below presents the Composition of Inconel 718.

Table 3.1. Composition of Inconel 718 (Wt.%) [100].

Element	Weight %
Ni	50.00 – 55.00
Cr	17.00 – 21.00
Nb	4.75 – 5.50
Mo	2.80 – 3.30
Ti	0.65 – 1.15
Al	0.20 – 0.80
Co	1.00
C	0.08
Mn	0.35
Si	0.35
P	0.015
S	0.015
B	0.006
Cu	0.30
Fe	Balance
Relative density	approx. 100 %
Density	min.8.15 g/cm³ min.0.294 b/in³

Removal of the casting faults of Inconel 718 is an expensive and long procedure [90]. The powder metallurgy (P/M) way is preferential because of overcoming these limitations on the processing of Inconel 718 [91]. In this study, Inconel 718 ® alloy powder has been used as the main material. The default particle size of the INCONEL® alloy 718 powder was 20 to 63 µm. It is a nickel based fine powdered heat resistant alloy with a standard density of 8,2 g/cm^3.The chemical combination of the INCONEL® alloy 718 powder is represented in Table 3.1. The techanical properties and technical data of the INCONEL® alloy 718 powder is represented in Table 3.2 and Table 3.3 below.

Table 3.2. Technical data of Inconel 718 (Wt.%) [101].

General Process Data	
Typical achievable part accuracy	
-small parts	approx. +/- 40 – 60 µm approx. +/- 1.6 – 2.4 x 10 -³ inch
- large parts	+/- 0.2 %
Min. wall thickness	typ. 0.3 - 0.4 mm typ. 0.012 – 0.016 inch
Surface roughness	
- after shot-peening	Ra 4 – 6.5 µm, Rz 20 - 50 µm Ra 0.16 – 0.25 x 10 -³ inch, Rz 0.78 – 1.97 x 10 -³ inch
- after polishing	Rz up to < 0.5 µm Rz up to < 0.02 x 10 -³ inch (can be very finely polished)
Volume rate	
- Parameter Set IN718_Performance (40 µm)	4 mm³/s (14.4 cm³/h) 0.88 in³/h

As shown the Table 3.2 above, according to past experiences dimensional precision for the geometries 40 µm when parameters able to be optimized for a specific rate of parts and 60 µm when building a new geometry. The geometry of the parts such as wall height affects the mechanical determination. Nonetheless, poly fast material has been used to hold the samples, as well as ethanol, and water has been used to clean the surface of samples. All materials have been supplied by the University of Wolverhampton, UK. Table 3.3 below presents the mechanical properties and heat treatment procedure of INCONEL® alloy 718 parts at at 20 °C (68 °F) [101].

Table 3.3. Mechanical properties of IN 718 parts [102].

Mechanical properties of parts at 20 °C (68 °F)			
	As built	**Heat treated per**	
		AMS 5662 [5]	**AMS 5664 [6]**
Tensile strength [7]			
horizontal direction (XY)	typ. 1060 ± 50 MPa (154 ± 7 ksi)		
vertical direction (Z)	typ. 980 ± 50 MPa (142 ± 7 ksi)	min. 1241 MPa (180 ksi) typ. 1400 ± 100 MPa (203 ± 15 ksi)	min. 1241 MPa (180 ksi) typ. 1380 ± 100 MPa (200 ± 15 ksi)
Yield strength (Rp 0.2 %) [7]			
horizontal direction (XY)	typ. 780 ± 50 MPa (113 ± 7 ksi)		
vertical direction (Z)	typ. 634 ± 50 MPa (92 ± 7 ksi)	min. 1034 MPa (150 ksi) typ. 1150 ± 100 MPa (167 ± 15 ksi)	min. 1034 MPa (150 ksi) typ. 1240 ± 100 MPa (180 ± 15 ksi)
Elongation at break [7]			
horizontal direction (XY)	typ. (27 ± 5) %		
vertical direction (Z)		170 ± 20 GPa 24.7 ± 3 Msi	170 ± 20 GPa 24.7 ± 3 Msi
Hardness	approx. 30 HRC approx. 287 HB	approx. 47 HRC approx. 446 HB	approx. 43 HRC approx. 400 HB

3.1.2 EOSINT M 270

The EOSINT M 270 which is shown in Figure 3.1 builds desired metal parts from 3D CAD data directly with direct metal laser sintering (DMLS) method. Direct metal laser sintering combines the metal powder into a solid part by melting the material powder focused on laser beam.

Figure 3.1. EOS M270 laser sintering machine

It's technical properties such a building volume, building speed and layer thicknesses are shown in Table 3.4 below. This system can build the highly complex geometric parts based on 3D CAD model without using any tooling in a few hours.

Table 3.4. Technical data of EOSINT M270 [103].

Technical Data of EOSINT M270	
Effective building volume (including building platform)	250mm x 250mm x 215mm
Building speed (material-dependent)	2 - 25 mm^3/s
Layer thickness (material-ependent)	20 - 60 µm
Laser type	Yb-fi bre laser, 200 W

3.2 EXPERIMENTAL PROCEDURE

In this study the M270 sintering system was used for building samples. The overall methodological summary of this study is described in Figure 3.2 below.

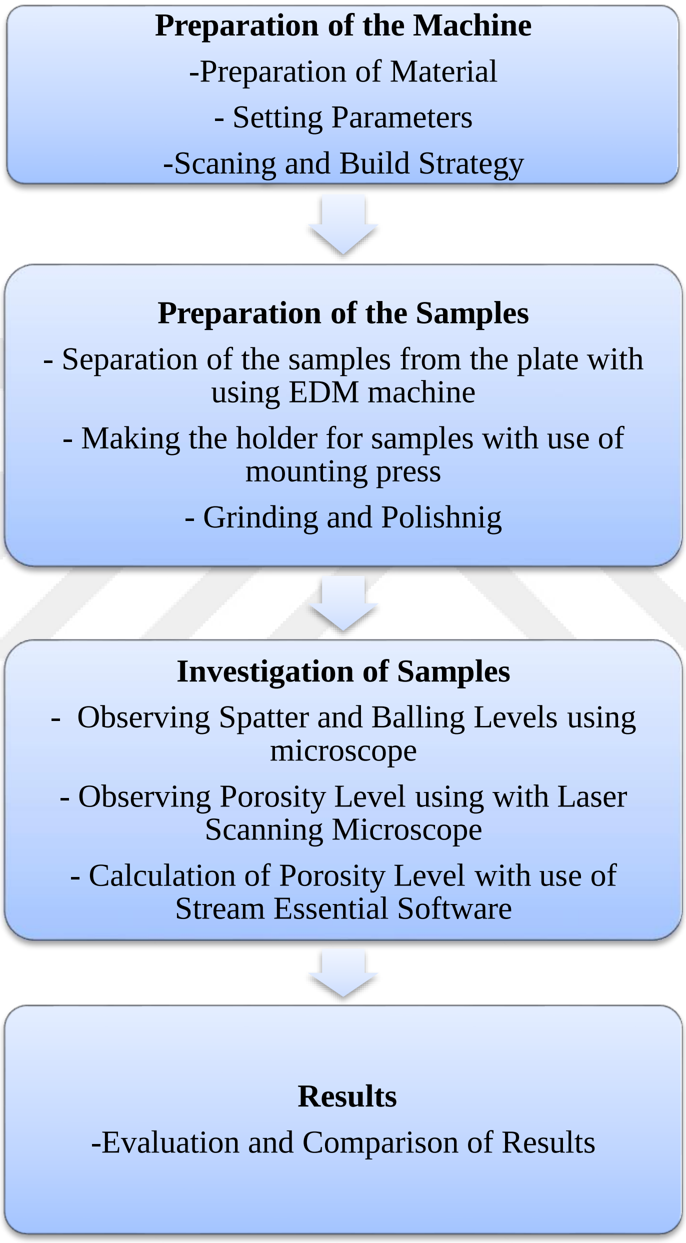

Figure 3.2. Process steps of this study.

The Inconel 718 powders were used to build 9 (multiple line samples) and 18 specimens with sizes of 12 mm × 12 mm × 5 mm which were used as test specimens. In this case, the machine is set in one of the preparatory stages of the appropriate parameters. There are spesific parameters for each material types. All experimental conditions were carried out based on various parameters of step over distances and scan speed. The aim of using this method was optimizing the process parameter of the laser melting of Inconel 718 as well as providing the best scan speed and step over distance parameters under constant and suitable laser power. At the same time, the parameters of scan speed and step over distance were the two controlled parameters, the porosity level and microstructures/contours on the test sample were the measured response of the samples surfaces. Table 3.5 below represents the settings in which the experiments were carried out. Various scan speed parameters were generated based on accepted Inconel 718 scan speed parameters.

Table 3.5. Experimental scan speed parameters of Inconel 718 on EOS M270.

Effect of Scan Speed			
Parts	**Scan Speed (mm/s)**	**Step over distance (mm)**	**Power (W)**
Part 1	900	2	195
Part 2	1000		
Part 3	1100		
Part 4	1200		
Part 5	1300		
Part 6	1400		
Part 7	1500		
Part 8	1600		
Part 9	1700		

Table 3.6. Experimental step over distance parameters of IN 718 on EOS M270.

Effect of Step Over Distance			
Parts	**Scan Speed (mm/s)**	**Step over distance (mm)**	**Power (W)**
Part 1	1400	0.05	195
Part 2		0.06	
Part 3		0.07	
Part 4		0.08	
Part 5		0.09	
Part 6		0.10	
Part 7		0.11	
Part 8		0.12	
Part 9		0.13	

The built samples based on Table 3.5 above were investigated with the use of microscope. Effect of balling and spatter on multiple lines samples (Sample 1, 2, 3, 4, 5 and 7) of Inconel 718 was observed which is presented Figure 4.1a,b,c,d and Figure 4.2a,b bellow. Furthermore, In Sample 6, 8 and 9 suitable surface without balling and spatter was observed as a result Sample 6 (Scan speed 1400 mm/s) was selected as a suitable scan speed value. In following Table 3.6 nine various step over distance values were created based on accepted Inconel 718 parameters. In the final step of setting parameters the original accepted EOS parameters (Part 1, Part 2, Part 3) were used and derived from experimental procedure parameters(Part 4, Part 5, Part 6) as well as new experimental parameters (Part 7, Part 8, Part 9) in the Table 3.7 below.

Table 3.7. Experimental parameters of Inconel 718 on EOS M270.

Effect of Scan speed and Step Over Distance			
Parts	**Scan Speed (mm/s)**	**Step over distance (mm)**	**Power (W)**
Part 1	1200	0.09	195
Part 2			
Part 3			
Part 4	1400	0.08	
Part 5			
Part 6			
Part 7	1300	0.08	
Part 8	1400	0.07	
Part 9	1500	0.08	

Equally for all the experiments, the power used was 195W and layer thickness was 20 micron.

3.2.1 Preperation of Samples

All samples were prepared separately for metagraphic investigation. As a first step, the electrical discharge machining (EDM) system was used for dividing samples from the plate thereafter, poly fast substance and mounting press machine were used which is shown below in Figure 3.3.

Figure 3.3. Automatic mounting press.

In this stage, eighteen samples were prepared for grinding and polishing steps.

3.2.2 Grinding and Polishing

The grinding of the samples was performed using the PEDEMAX-2 grinding machine which is shown below Figure 3.4.

Figure 3.4. PEDEMAX-2 grinding machine

Different grinding papers with abrasive grit numbers P220, P500, P1200 were used respectively.

Figure 3.5. Universal polisher machine.

After grinding process, the eighteen samples were polished using a Universal polisher machine which is shown Figure 3.5 above. The Universal Polisher Machine has two partitions as 6 micron and 1 micron. In the first instance, the 6 micron partition on the universal polisher was used to polish whole samples afterwards the samples were placed on the 1 micron partition on the universal polisher machine for a precision polish. After this process the samples were washed with water and a ethanol. This process was continued until whole surface reached the required quality.

3.3 APPRAISAL

After the polishing step, all the polished test samples were checked for their porosity and microstructures with use of a laser scanning microscope shown in Figure 3.6 below.

Figure 3.6. OLYMPUS - OLS300 Laser scanning microscope.

Two focusing strategies which are shown below Figure 3.7.a and Figure 3.7.b were used for examining the sufficient surface range with the stings of TV view and focal (CF) turn on, photographs were taken. When examining the samples in Table 3.6 above; sample 3, 4 and 5 were found to be close to the desired results. Therefore, three samples (Sample 3,4 and 5 were investigated with larger mega pixel as well as compared with each other according to surface quality. Then images were saved as JPEG file format.

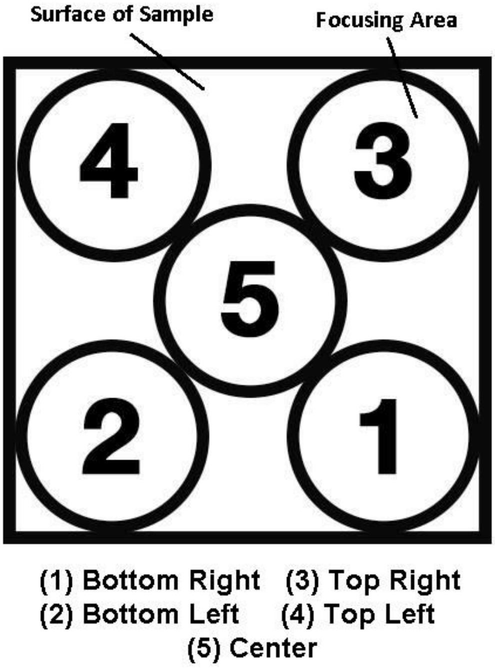

(a)

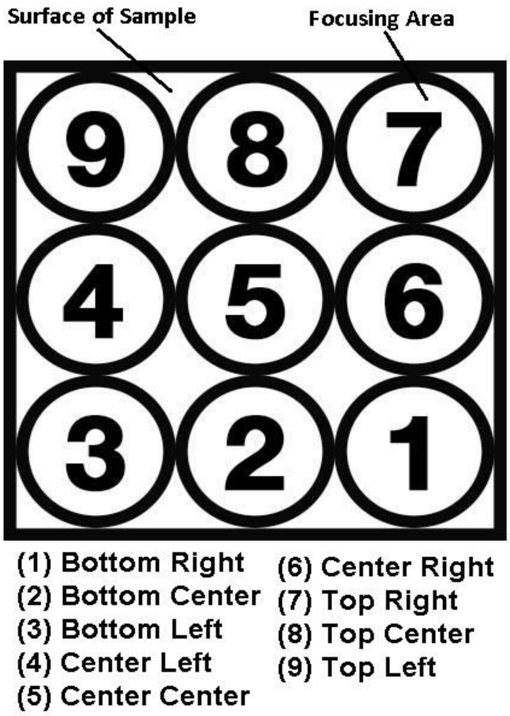

(b)

Figure 3.7. (a) Focusing of table 3.6 and (b) Focusing of table 3.7.

Finally, the stream essentials software was used to obtain porosity data from images. The Olympus Microscope on 5x is 2560 by 1920 μm and the size of saved images 1024 x 768 μm for this reason the formulation below was applied for to calibrate all images. For x axis: 2560 / 1024 = 2,5 μm and For y axis: 1920 / 768 = 2,5 μm (μm /pixels). In this manner, The percentage of porosity level of all images were calculated and documented separately with Stream Essential software.

PART 4

RESULTS AND DISCUSSION

4.1 EXPERIMENTAL RESULTS

4.1.1 Effect of Scan Speed Parameters on Multiple Lines Samples

Tests were made ın order to generate elements of the samples wıth the use of dıfferent scan speed parameters while keeping the laser power same at 195W and step over distance at 2mm. Result of the test is shown in Table 4.1 and Figure Figure 4.1a,b,c,d, Figure 4.2a,b and Figure 4.2a,b below.

a) Part 1 (scan speed-900)

b) Part 2 (scan speed-1000)

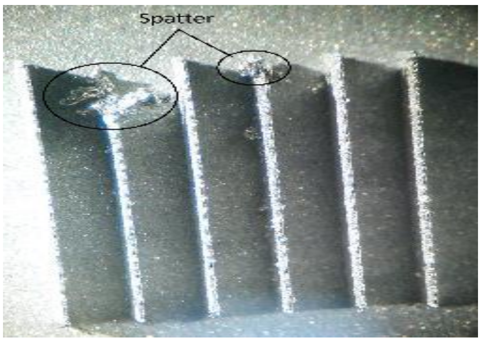

c) Part 3 (scan speed-1100)

d) Part 4 (scan speed-1200)

Figure 4.1. (a,b,c,d) Effects of balling and spatter on multiple lines samples.

Effects of Balling and Spatter on Multiple Lines Samples of Inconel 718 were observed as well as the regions of balling and spatter was marked in Figure 4.1a,b,c,d and Figure 4.2a,b.

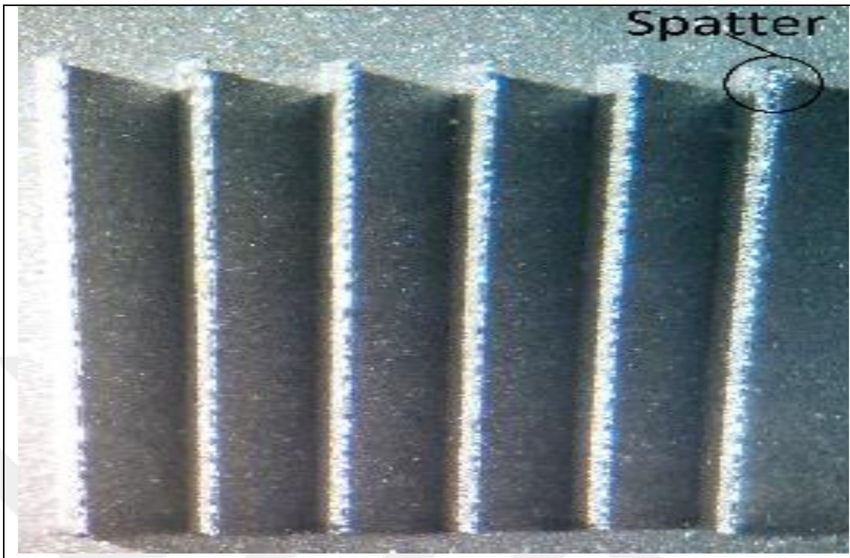

a) Part 5 (scan speed-1300)

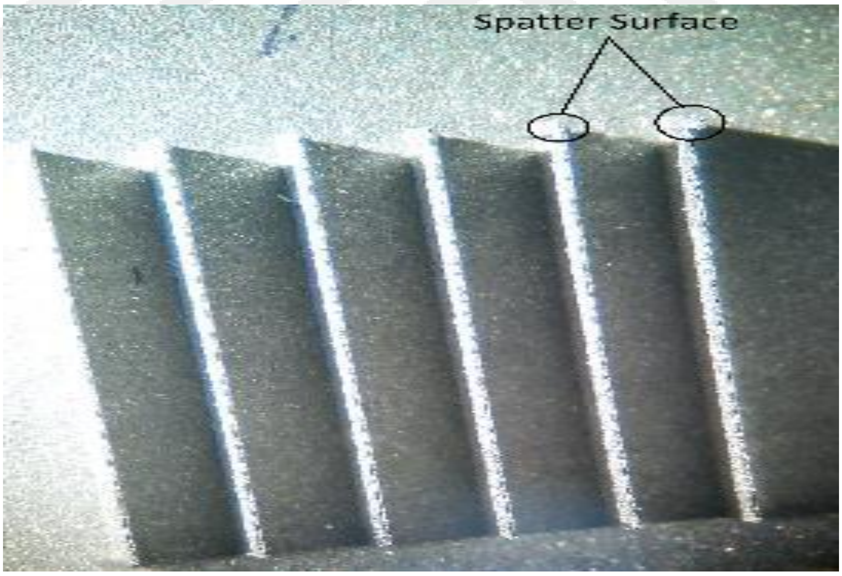

b) Part 7 (scan speed-1500)

4.2. (a,b) Effects of spatter on multiple lines samples of Inconel 718.

In Sample 1 (Scan speed 900 mm/s),Sample 2 (Scan speed 1000 mm/s),Sample 3 (Scan speed 1100 mm/s),Sample 4 (Scan speed 1200 mm/s) rough regions balling and spatter occurred. However, In Sample 5 (Figure 4.1a) and Sample 7 (Scan speed 1500 mm/s) regions of spatter were observed.

a) Part 6 (scan speed-1400)

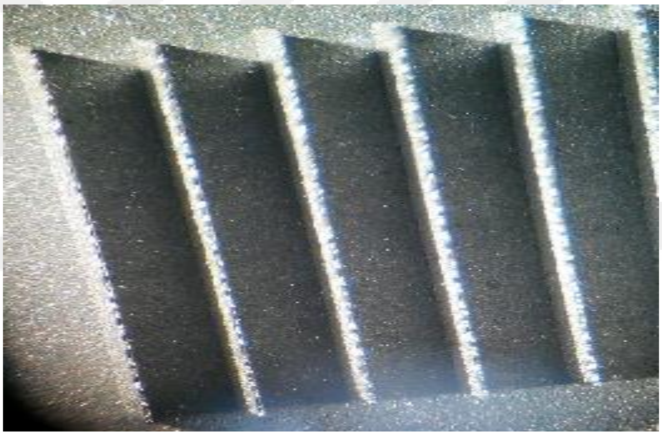

b) Part 8 (scan speed-1600)

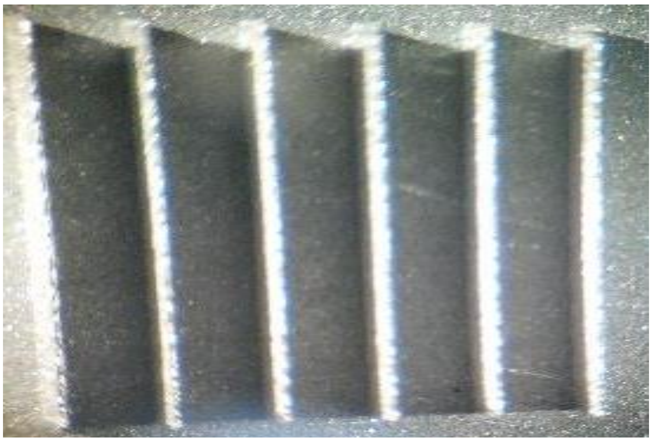

c) Part 9 (scan speed-1700)

Figure 4.1. (a,b,c) Suitable surface having samples of Inconel 718.

On the other hand, In Sample 6, sample 8 and sample 9 shown in Figure 4.3.a,b,c suitable surface without balling or spatter impacts was observed. Based on the acquired images, Sample 6 see Figure 4.3.a was found to have the best ideal surface quality at the same time sample 1 see Figure 4.1.a was found have the worst surface quality.

Table 4.1. Results for effect of scan speed on multiple lines samples of IN 718.

Effect of Scan Speed on Multiple Lines Samples			
Parts	**Scan Speed (mm/s)**	**Step over distance (mm)**	**Effects on the Surface**
Part 1	900		Balling and Spatter
Part 2	1000		Balling and Spatter
Part 3	1100		Balling and Spatter
Part 4	1200		Balling and Spatter
Part 5	1300	2	Spatter
Part 6	**1400**		**Suitable surface**
Part 7	1500		Spatter
Part 8	**1600**		**Suitable surface**
Part 9	**1700**		**Suitable surface**

In this manner, 1400 mm/s was considered as the best scan speed setting for material of Inconel 718 on EOS M270 Laser Melting Machine.

4.1.2 Effect of Step over Distance Parameters on Generated Samples

After a suitable scan speed is determined (1400 mm/s), various step over distance parameters from (0.05 to 0.13 mm) were generated based on accepted Inconel 718 step over distance parameters. According to those step over distance parameters Table 3.6 above, nine Inconel 718 samples were built on EOS M270 Laser Melting Machine which are shown Figure 4.4 below. After the samples were removed from the plate, all samples were prepared for investigating on the Laser scanning microscope. However, microscopic photographs of each sample were taken separately according to focusing strategy at Figure 3.7a. Nine samples produced with different step over parameters and all of the images have been taken from microscope of laser scanning. Furthermore, In the Figure 4.5 to Figure 4.13 below, all images were investigated for porosity level on steam essential software.

Figure 4.2. Inconel 718 samples made with different step over parameters.

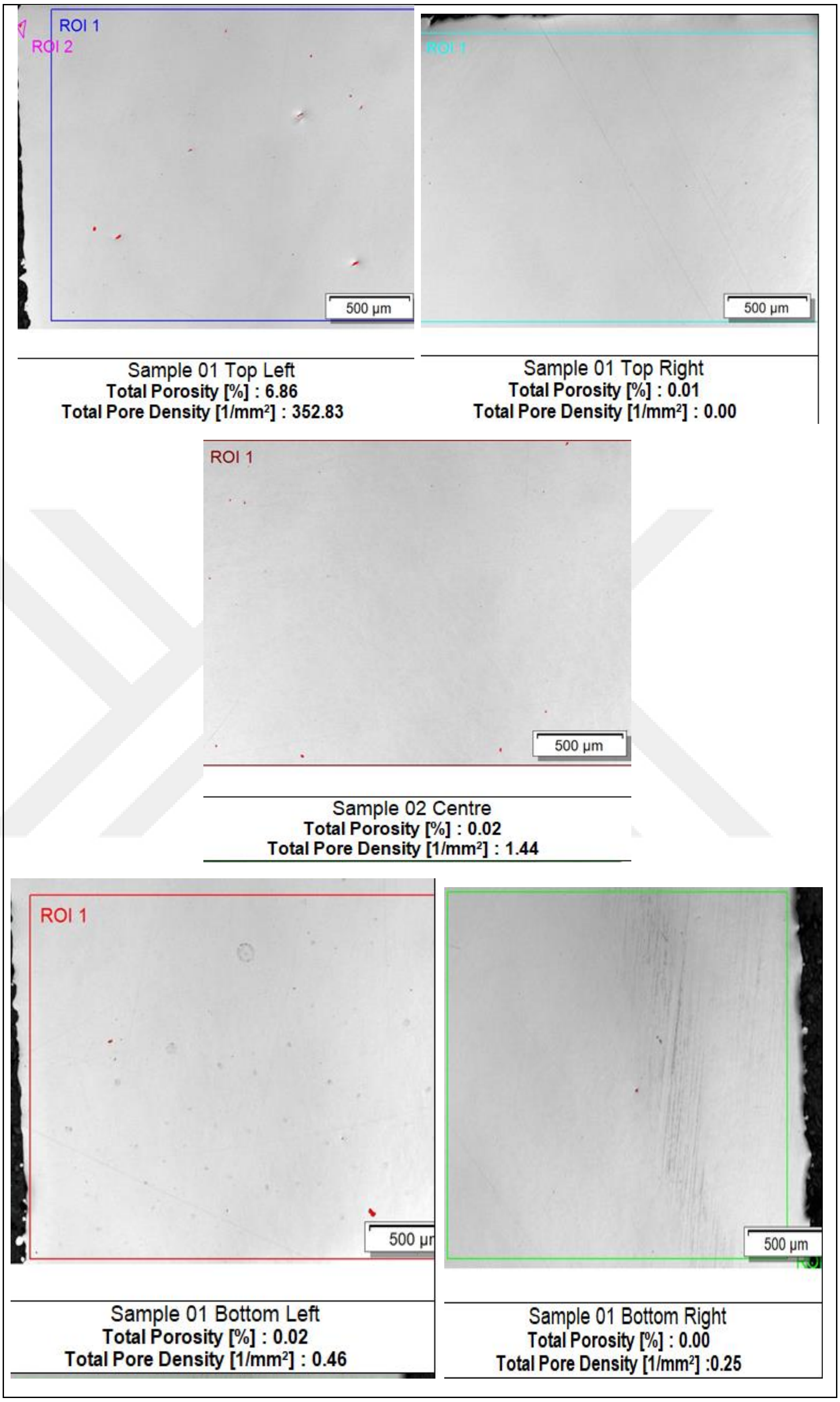

Figure 4.3. Inconel 718 sample 1.

Sample 1 has been created using step over distance 0.05. The porosity level is shown in Figure 4.3 above.

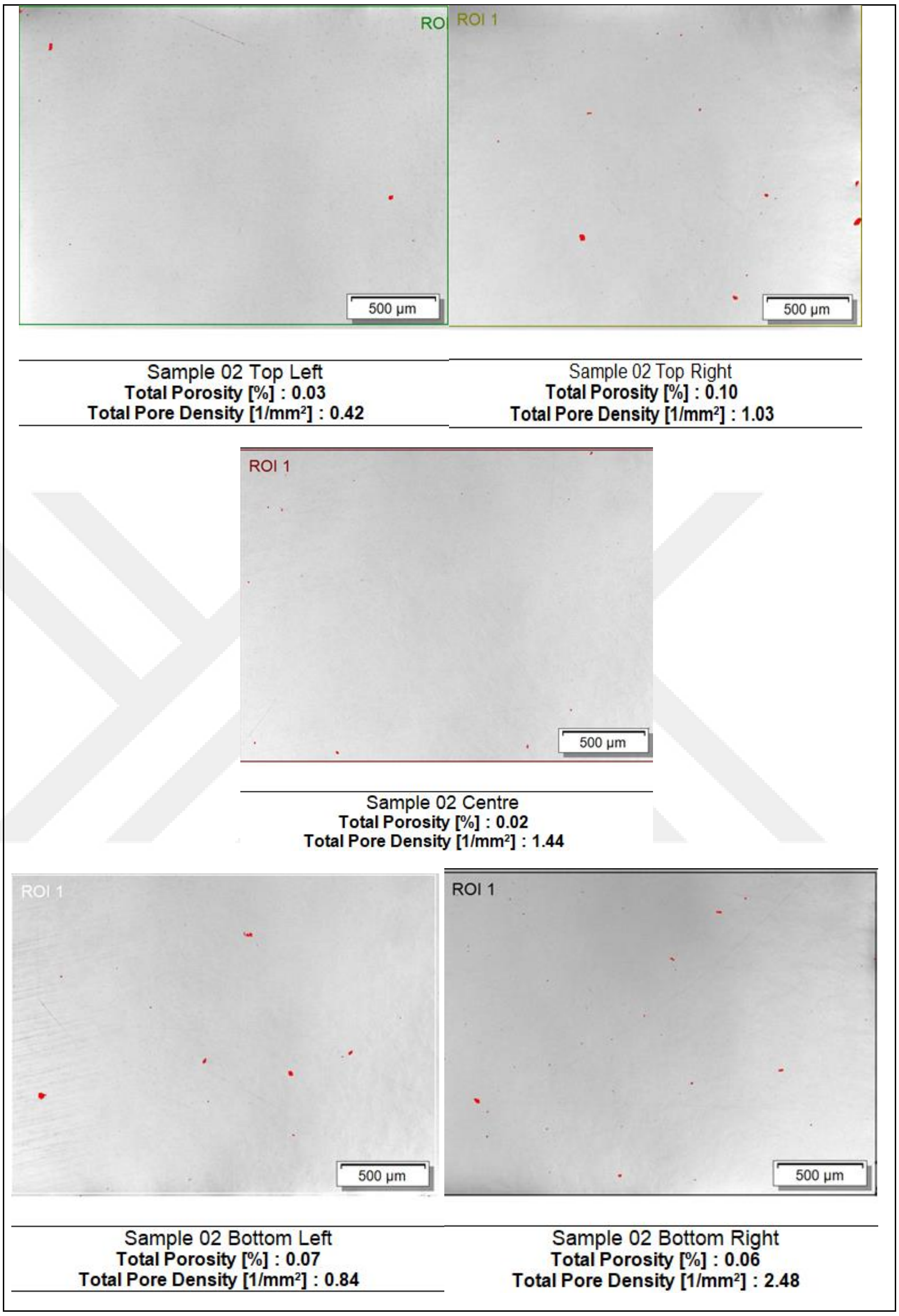

Figure 4.4. Inconel 718 sample 2.

Sample 2 has been created using Step Over Distance 0,06. The porosity level is shown in Figure 4.4. above.

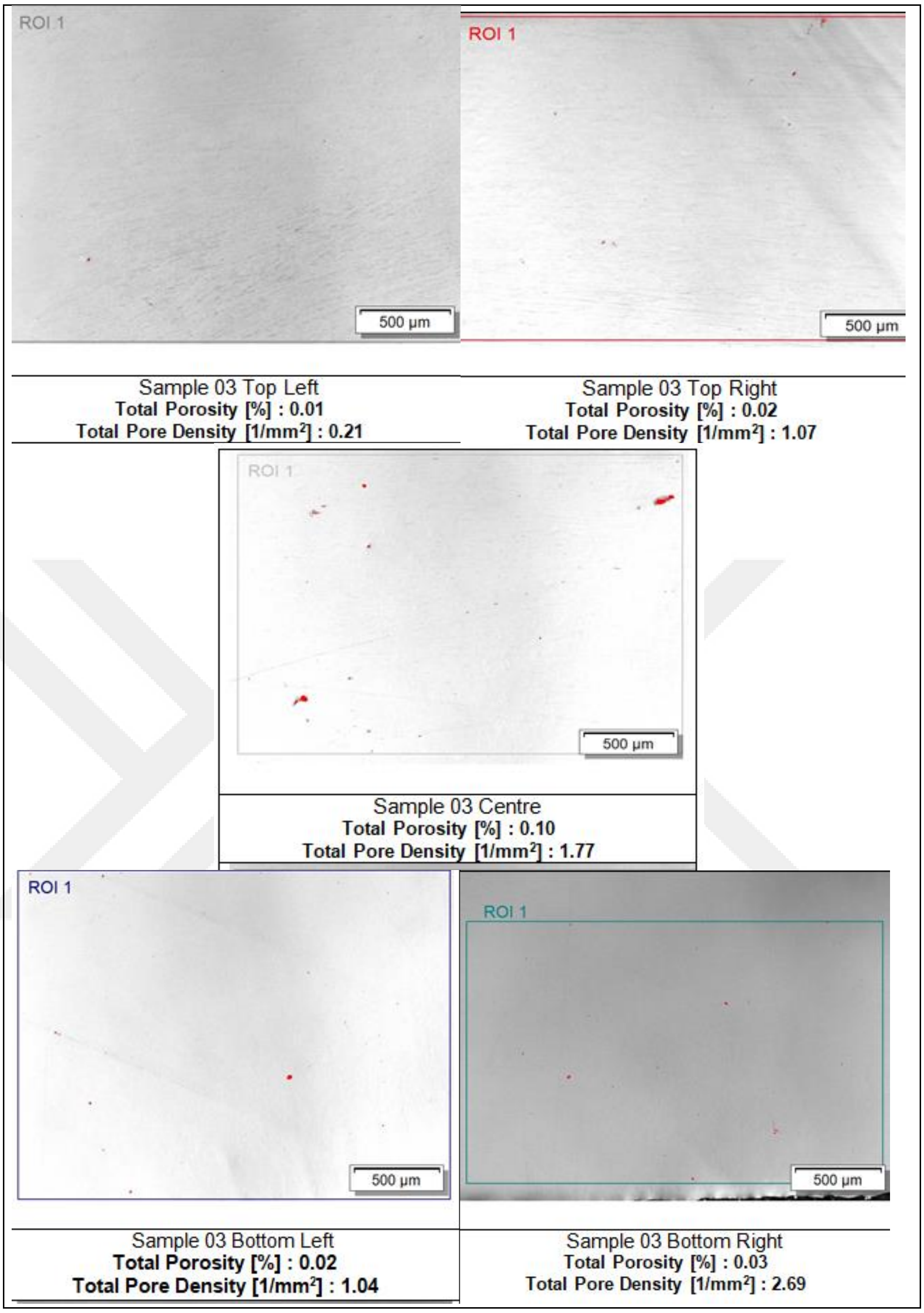

Figure 4.5. Inconel 718 sample 3.

Sample 3 has been created using step over distance 0,07. The porosity level is shown in Figure 4.5. above.

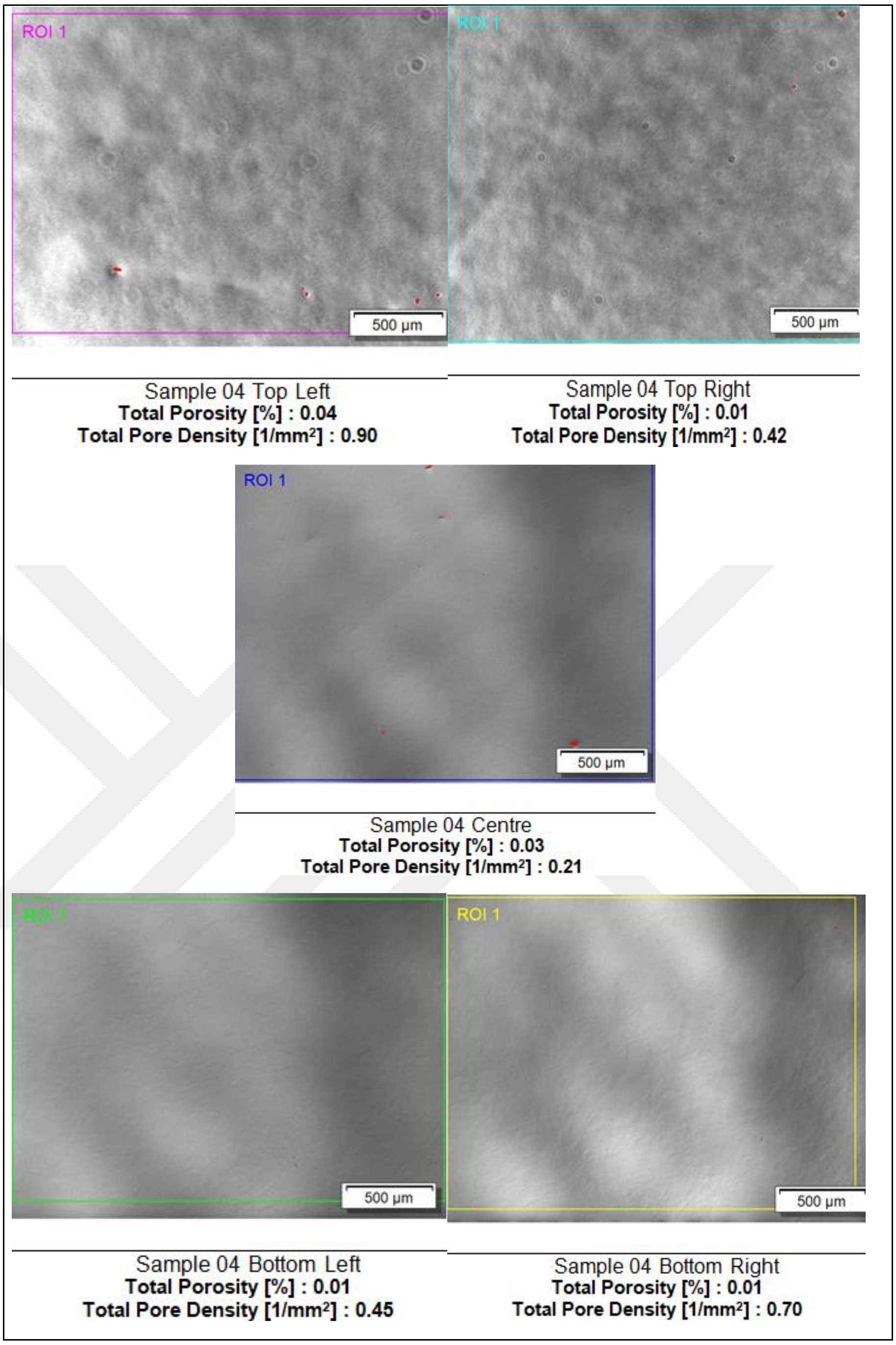

Figure 4.6. Inconel 718 sample 4.

Sample 4 has been created using step over distance 0,08. The porosity level is shown in Figure 4.6. above.

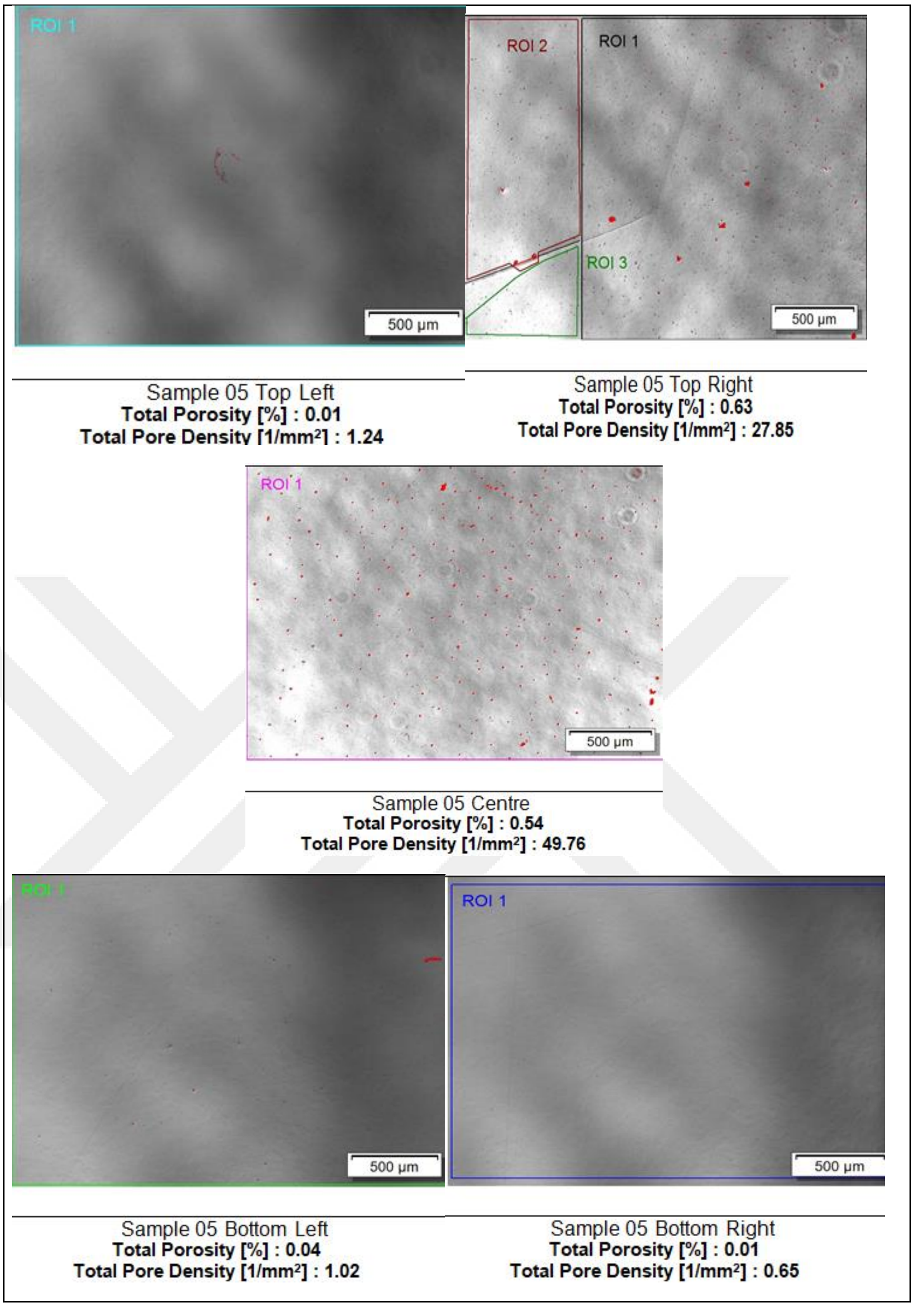

Figure 4.7. Inconel 718 sample 5.

Sample 5 has been created using step over distance 0,09. The porosity level is shown in Figure 4.7. above.

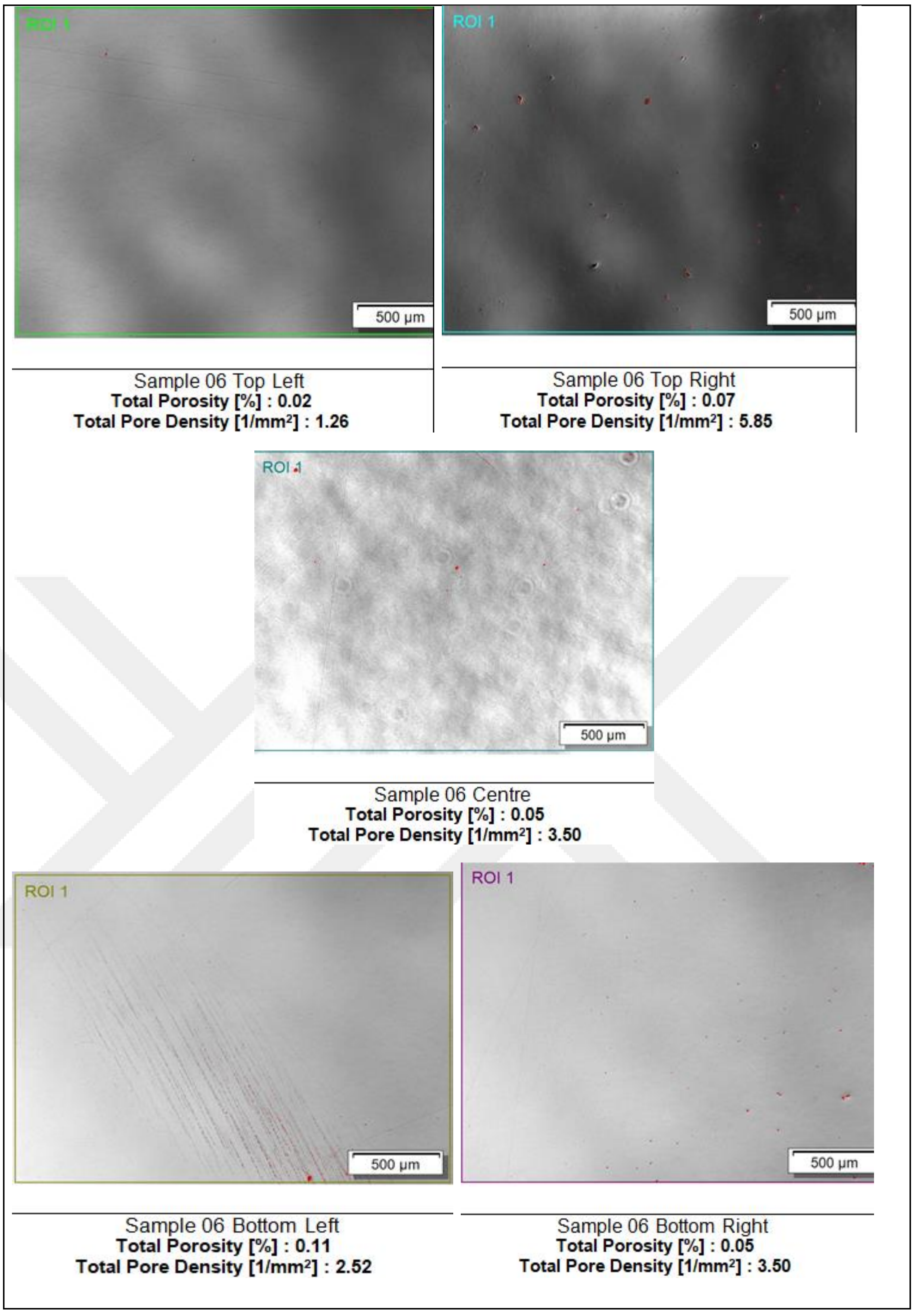

Figure 4.8. Inconel 718 sample 6.

Sample 6 has been created using step over distance 0,10. The porosity level is shown in Figure 4.8. above.

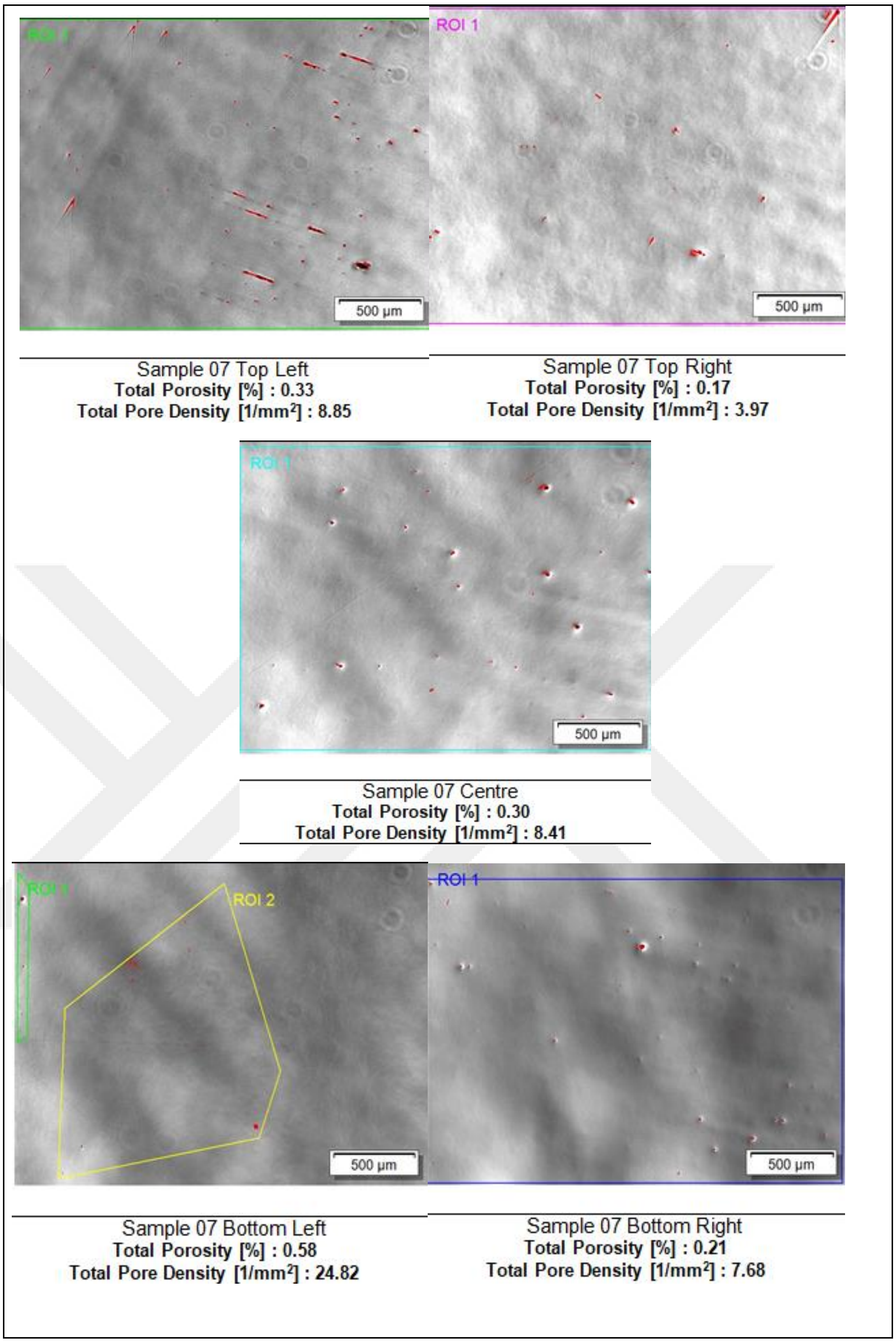

Figure 4.9. Inconel 718 sample 7.

Sample 7 has been created using step over distance 0,11. The porosity level is shown in Figure 4.9. above.

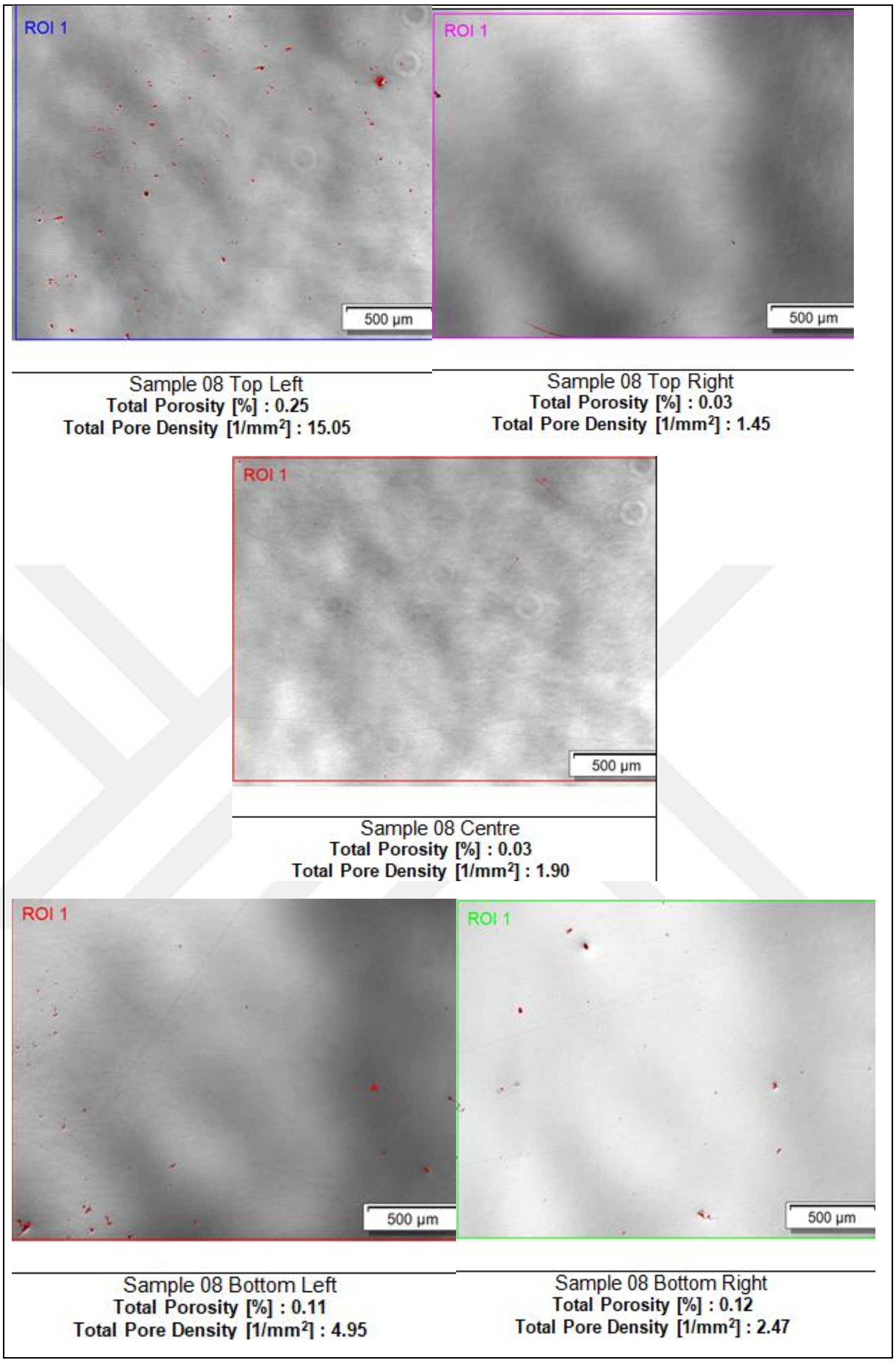

Figure 4.10. Inconel 718 sample 8.

Sample 8 has been created using step over distance 0,12. The porosity level is shown in Figure 4.10. above.

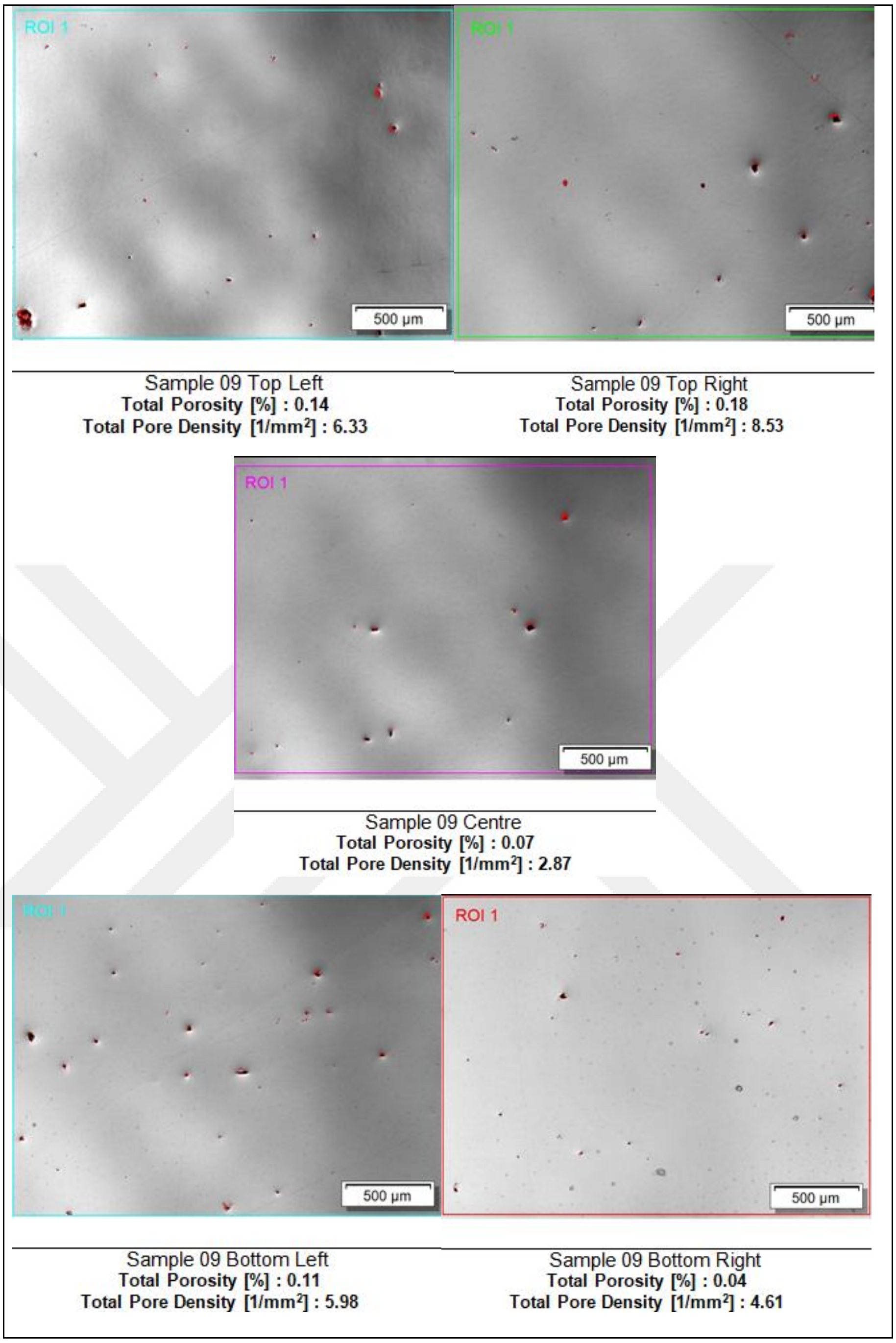

Figure 4.11. Inconel 718 sample 9.

Sample 9 has been created using step over distance 0,13. The porosity level is shown in Figure 4.11. above.

Table 4.2. Porosity values of Inconel 718 samples for various step over parameters.

Step Over Distance (mm)	Average Porosity Level [%]		Average Pore Density Level [1/mm^2]	
	Porosity	Standard Deviation	Pore Density	Standard Deviation
0.05	6.99	3.06	353.54	157.71
0.06	0.28	0.001	6.21	0.78
0.07	0.18	0.03	6.78	0.92
0.08	0.10	0.41	2.68	0.26
0.09	1.23	0.31	80.52	22.12
0.10	0.3	0.03	16.63	1.68
0.11	1.42	0.18	49.76	8.85
0.12	0.54	0.09	25.82	5.68
0.13	0.54	0.05	28.32	2.10

Table 4.2. above represents the porostiy level and pore density deviations for each step over distance.

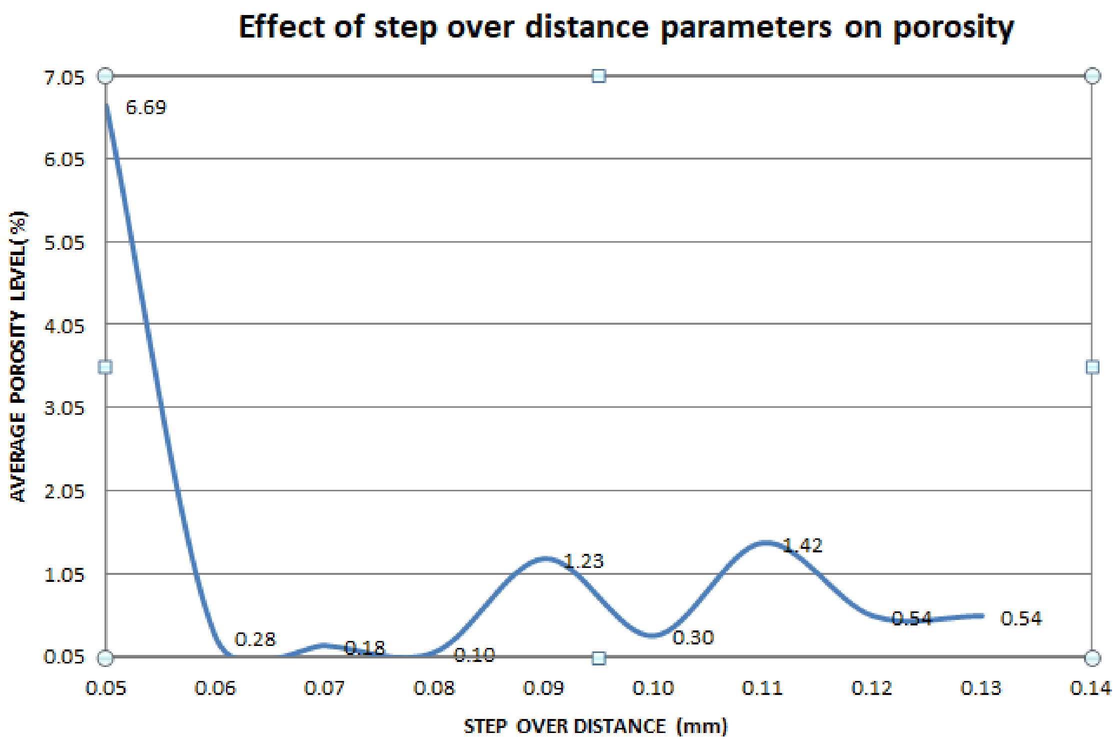

Figure 4.12. Effect of step over distance parameters on porosity.

Figure 4.12. above represents effect of step over distance parameters on porosity for each step over distance.

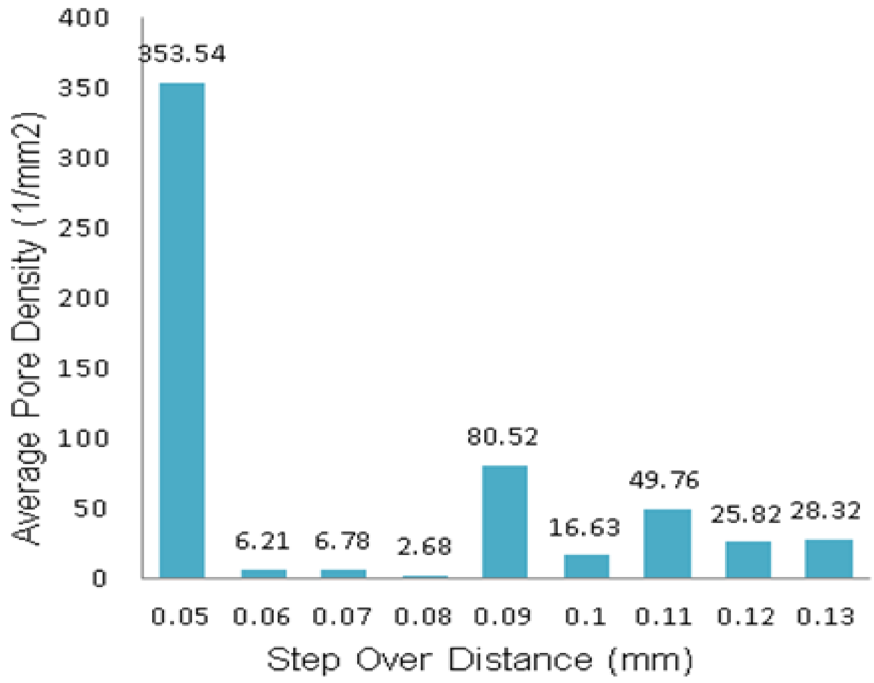

Figure 4.13. Effect of step over distance parameters on pore density

Pore density levels and percentage of porosity levels of each sample along with the standard deviation are given in the Table4.2 above. According to information of Table 4.2, the percentage of porosity range is 0,10% to 6,99% (minimum to max) also standard deviation value is 0,41 to 3,06 respectively. In addition to, effect of step over distance parameters on pore density levels are shown in Figure 4.15 above.

The most porosity level was seen at step over distance of 0,05 mm however the least porosity level was seen at step over distance of 0,8 mm which is presents Figure 4,14 above. In this manner, the step over distance of 0,08 mm and scan speed of 1400 mm/s are optimal parameters for Inconel 718 on the EOS M270 laser melting machine.

4.1.3 Effect of the Parameters on Generated Samples

In this stage, parameters of Table 4.3 were built then microscopic photographs of each sample were taken separately according to focusing strategy at Figure 3.7.b.

Table 4.1. Official accepted EOS, chosen optimal and experimental parameters.

<table>
<tr><th>Parts</th><th>Scan Speed (mm/s)</th><th>Step over distance (mm)</th><th>Power (W)</th></tr>
<tr><td>Part 1</td><td rowspan="3" colspan="2">1200 0.09
(Official Accepted EOS Parameters)</td><td rowspan="9">195</td></tr>
<tr><td>Part 2</td></tr>
<tr><td>Part 3</td></tr>
<tr><td>Part 4</td><td rowspan="3" colspan="2">1400 0.08
(Chosen Optimal Parameters)</td></tr>
<tr><td>Part 5</td></tr>
<tr><td>Part 6</td></tr>
<tr><td>Part 7</td><td>1.300</td><td>0.08</td></tr>
<tr><td>Part 8</td><td>1400</td><td>0.07</td></tr>
<tr><td>Part 9</td><td>1500</td><td>0.08</td></tr>
</table>

Nine samples were produced with different scan speed and step over parameters then all of the images have been taken with use of laser scanning microscope. Furthermore, In the Images 4.6.1 to Figure 4.6.9 below, all images was investigated for porosity level on steam essential software.

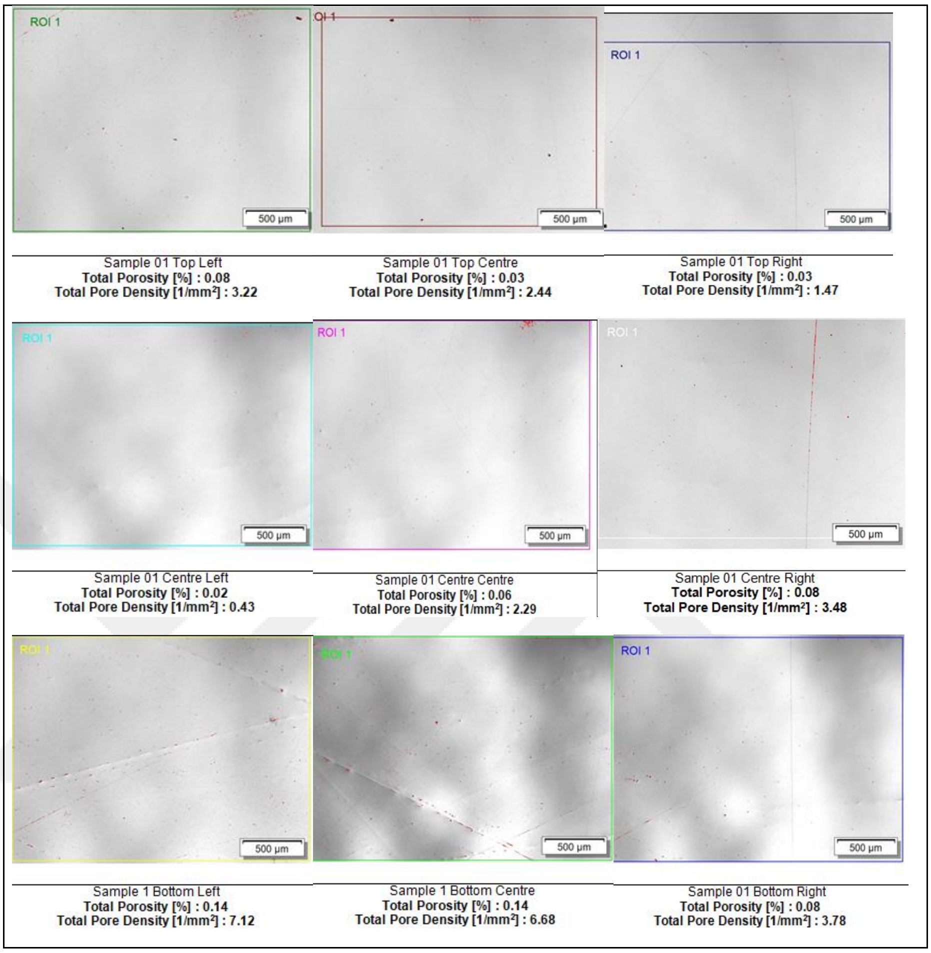

Figure 4.14. Inconel 718 sample 1.

Sample 1 has been created using scan speed - 1200 and step over distance – 0,09. The porosity level is shown for each area in Figure 4.14 above.

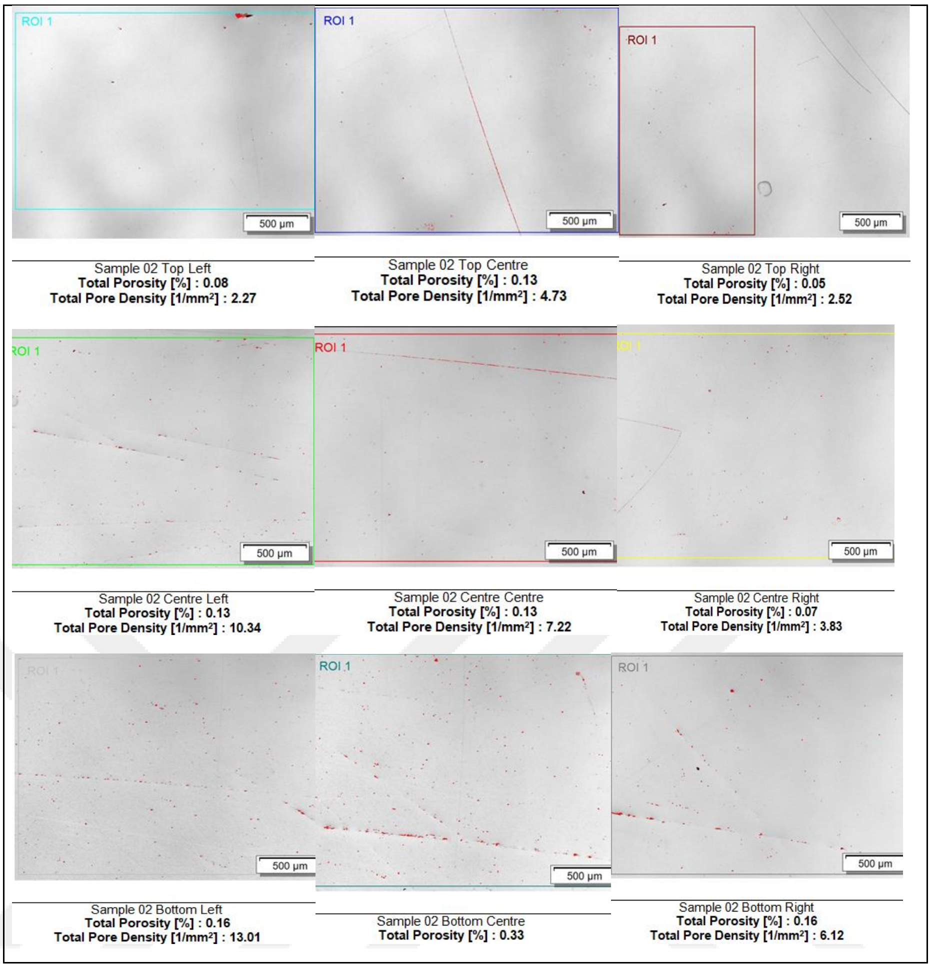

Figure 4.15. Inconel 718 sample 2.

Sample 2 has been created using scan speed - 1200 and step over distance – 0,09. The porosity level is shown for each area in Figure 4.15. above.

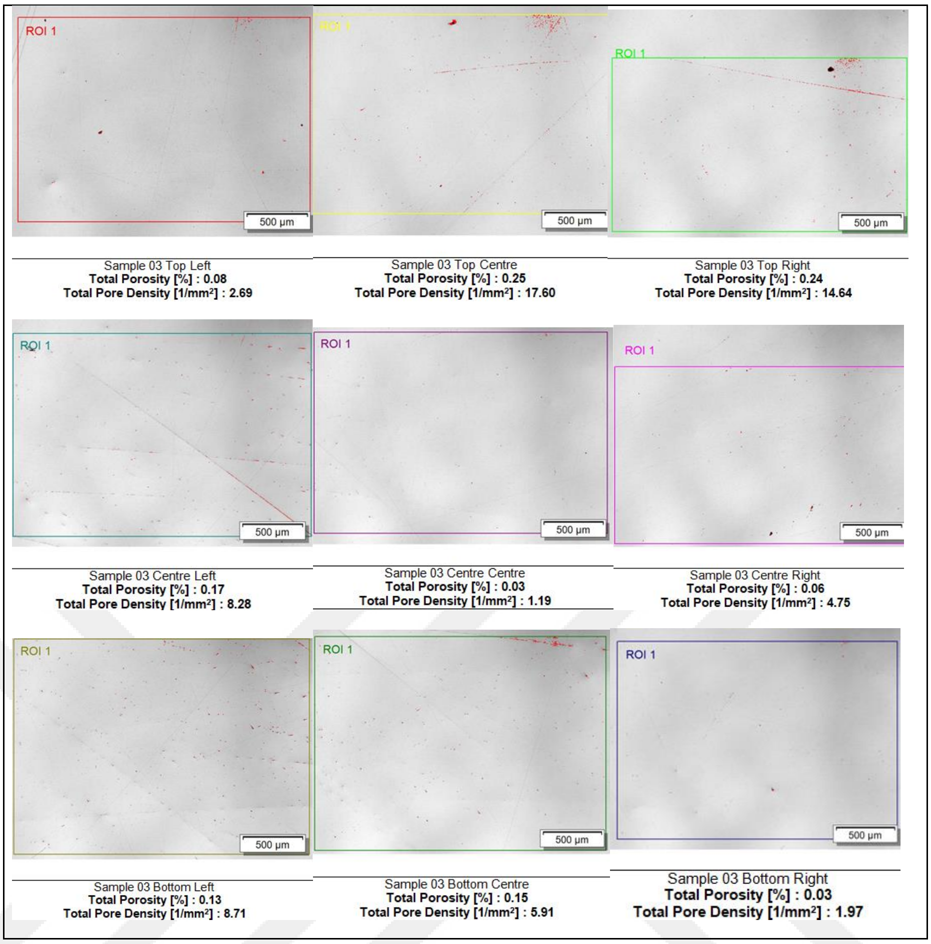

Figure 4.16. Inconel 718 sample 3.

Sample 3 has been created using scan speed - 1200 and Step over distance – 0,09. The porosity level is shown for each area in Figure 4.16 above.

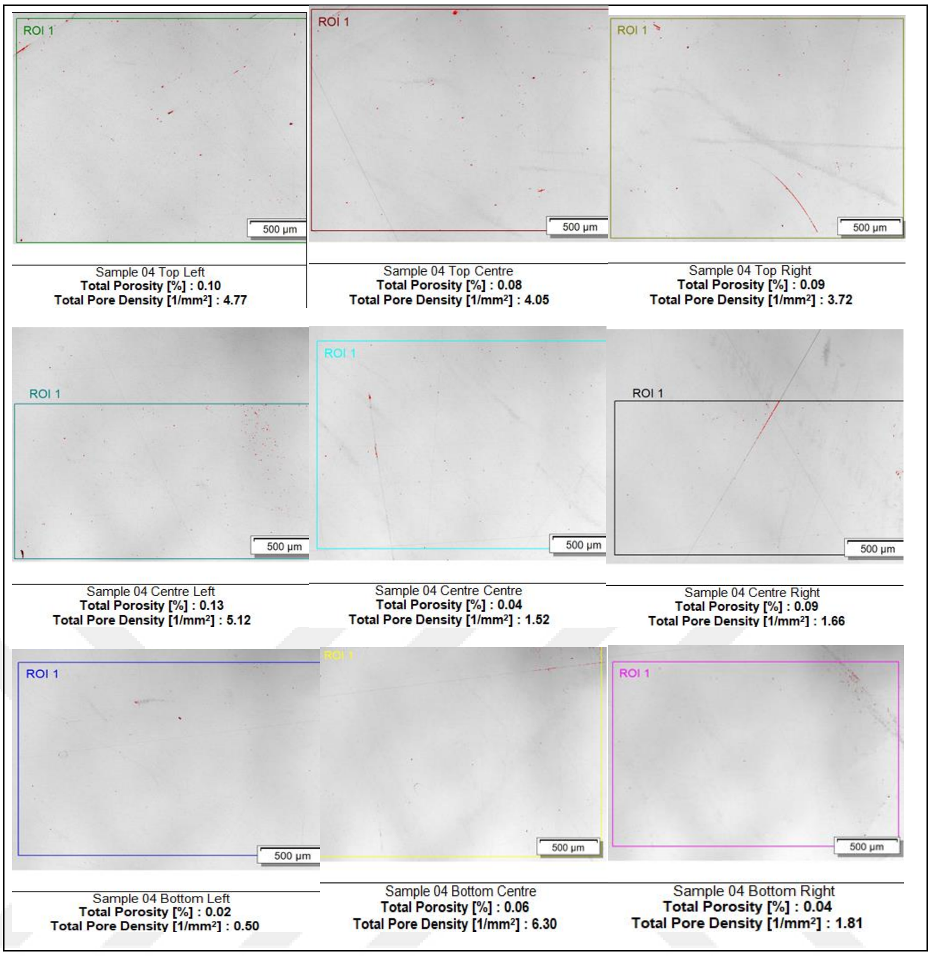

Figure 4.17. Inconel 718 sample 4.

Sample 4 has been created using scan speed - 1400 and step over distance – 0,08. The porosity level is shown for each area in Figure 4.17. above.

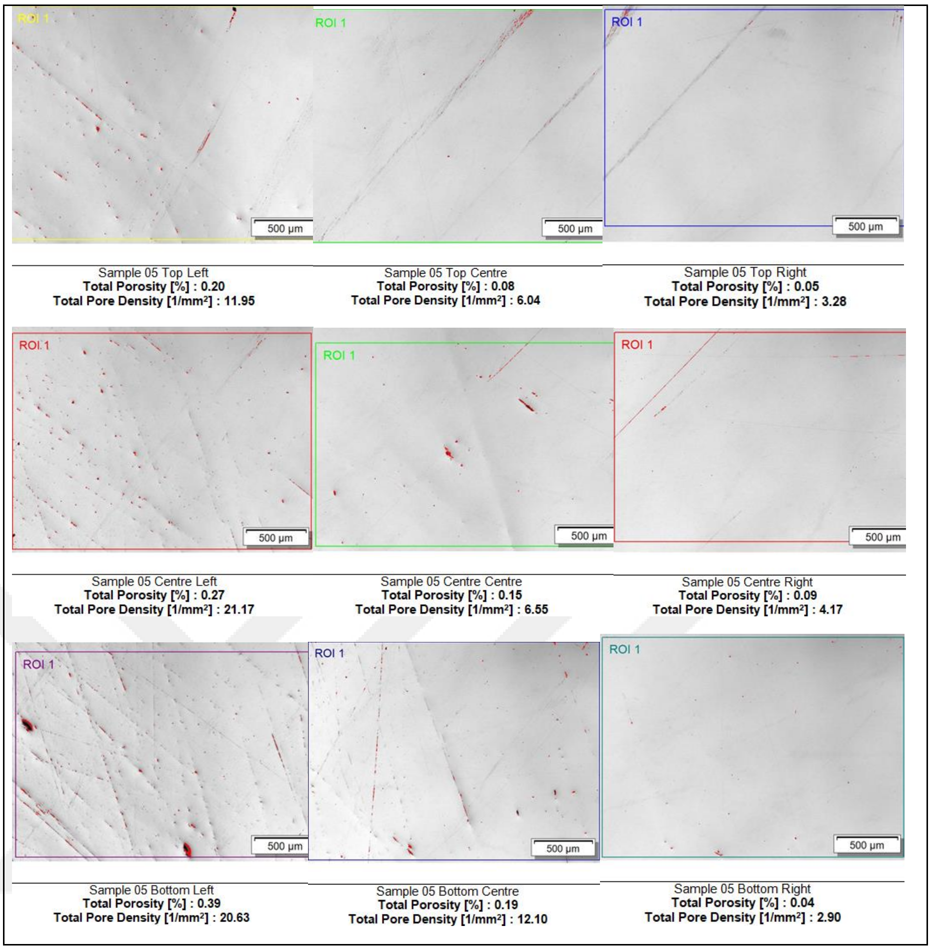

Figure 4.18. Inconel 718 sample 5.

Sample 5 has been created using scan speed - 1400 and step over distance – 0,08. The porosity level is shown for each area in Figure 4.20. above.

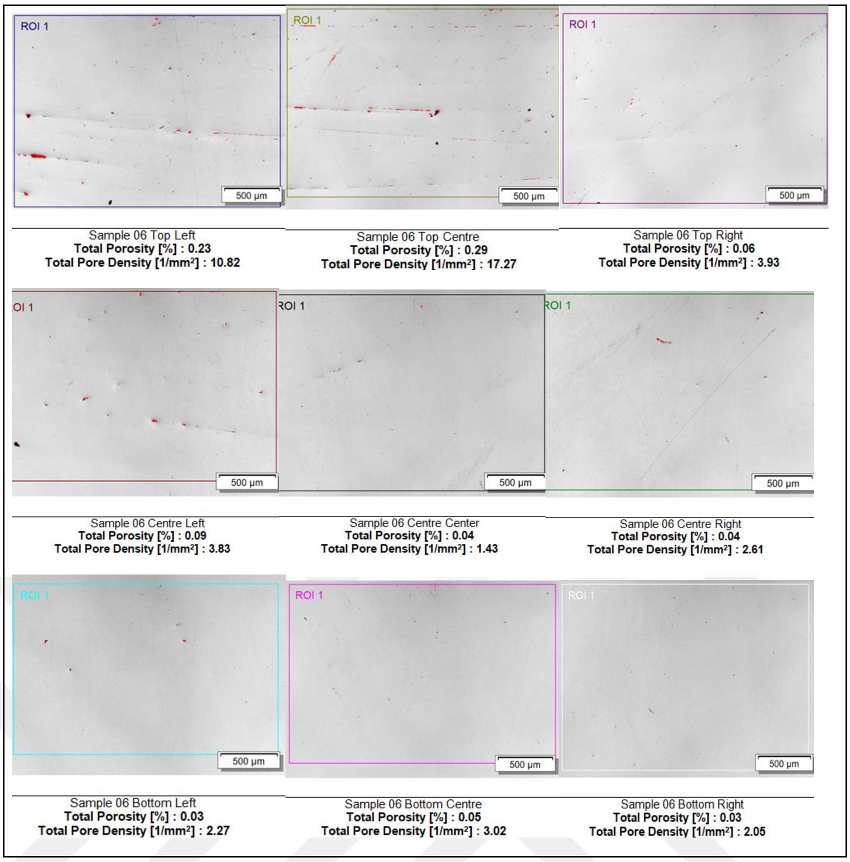

Figure 4.19. Inconel 718 sample 6.

Sample 6 has been created using scan speed - 1400 and step over distance – 0,08. The porosity level is shown for each area in Figure 4.19. above.

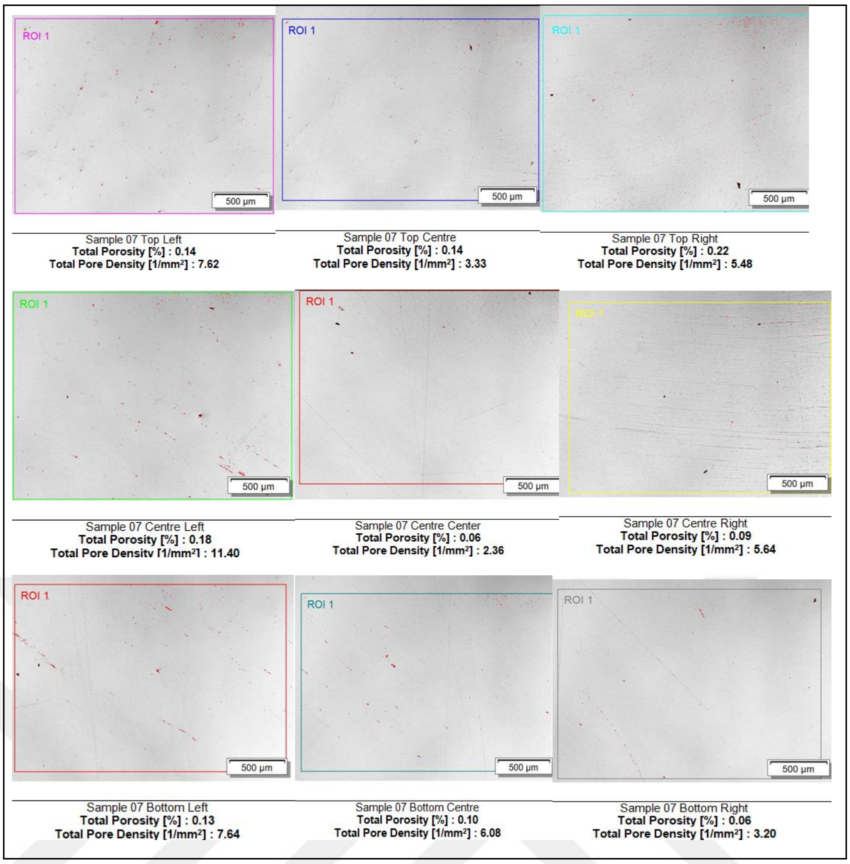

Figure 4.20. Inconel 718 sample 7.

Sample 7 has been created using scan speed - 1300 and step over distance – 0,08. The porosity level is shown for each area in Figure 4.20. above.

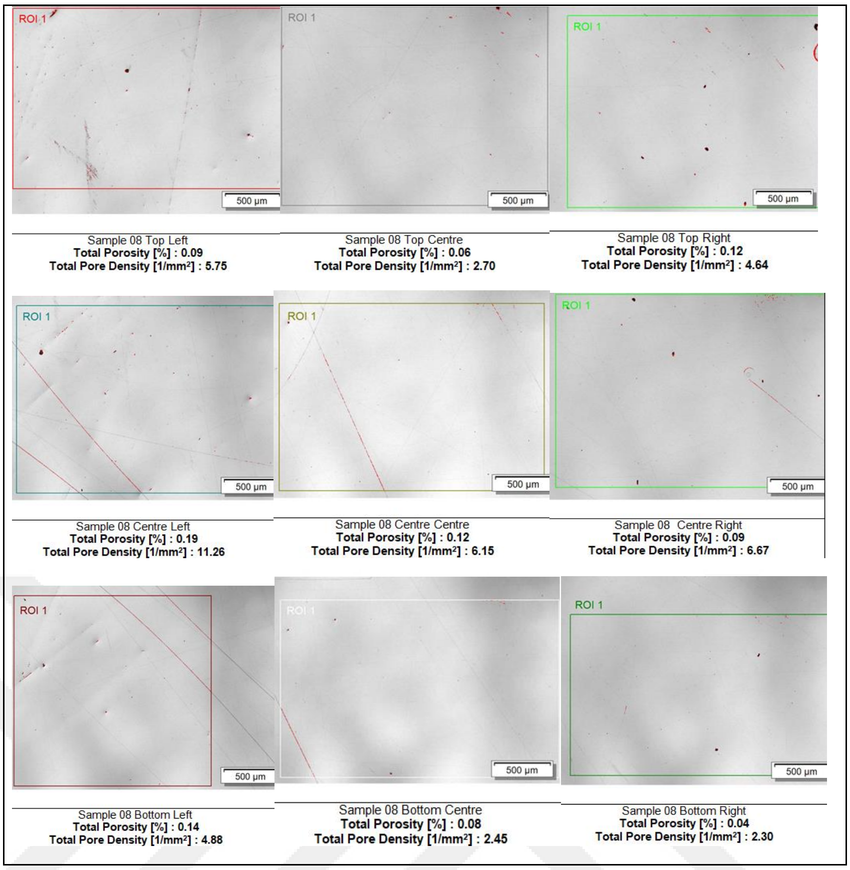

Figure 4.21. Inconel 718 sample 8.

Sample 8 has been created using scan speed - 1400 and step over distance – 0,07. The porosity level is shown for each area in Figure 4.21. above.

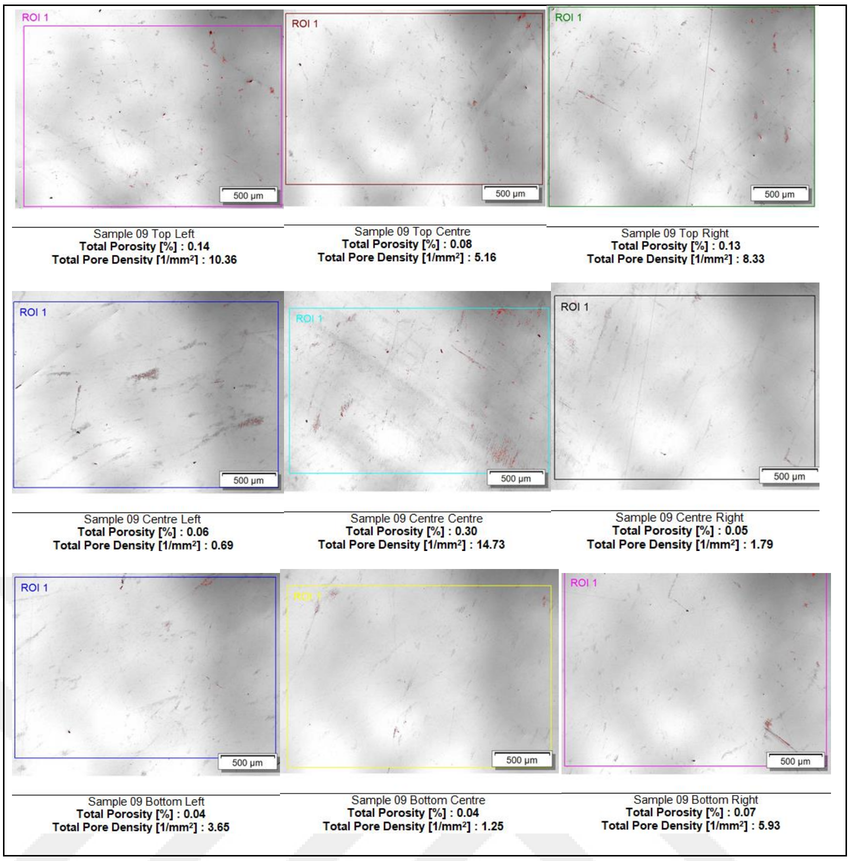

Figure 4.22. Inconel 718 sample 9.

Sample 9 has been created using scan speed - 1500 and step over distance – 0,08. The porosity level is shown for each area in Figure 4.22. above.

Areas of Sample 1	Average Porosity Level [%]	
	Porosity	Standard Deviation
Bottom Center	0.14	
Bottom Left	0.14	
Bottom Right	0.08	
CenterCenter	0.06	
Center Left	0.02	
Center Right	0.08	
Top Center	0.03	
Top Left	0.08	
Top Right	0.03	
TOTAL	0.66	0.044441

a)

Areas of Sample 2	Average Porosity Level [%]	
	Porosity	Standard Deviation
Bottom Center	0.33	
Bottom Left	0.16	
Bottom Right	0.16	
CenterCenter	0.13	
Center Left	0.13	
Center Right	0.07	
Top Center	0.13	
Top Left	0.08	
Top Right	0.05	
TOTAL	1.24	0.0819722

b)

Areas of Sample 3	Average Porosity Level [%]	
	Porosity	Standard Deviation
Bottom Center	0.15	
Bottom Left	0.13	
Bottom Right	0.03	
CenterCenter	0.03	
Center Left	0.17	
Center Right	0.06	
Top Center	0.25	
Top Left	0.08	
Top Right	0.24	
TOTAL	1.14	0.0835165

c)

Figure 4.23. Inconel 718 samples a) 1 b) 2 c) 3 total porosity level.

Figure 4.23. above represents the total porosity level using officially accepted EOS scan speed and step over parameters on Inconel 718 samples a) 1 b) 2 c) 3.

Areas of Sample 4	Average Porosity Level [%]	
	Porosity	Standard Deviation
Bottom Center	0.06	
Bottom Left	0.02	
Bottom Right	0.04	
CenterCenter	0.04	
Center Left	0.13	
Center Right	0.09	
Top Center	0.08	
Top Left	0.1	
Top Right	0.09	
TOTAL	0.65	0.0349205

a)

Areas of Sample 5	Average Porosity Level [%]	
	Porosity	Standard Deviation
Bottom Center	0.19	
Bottom Left	0.39	
Bottom Right	0.04	
CenterCenter	0.15	
Center Left	0.27	
Center Right	0.09	
Top Center	0.08	
Top Left	0.2	
Top Right	0.05	
TOTAL	1.46	0.1147582

b)

Areas of Sample 6	Average Porosity Level [%]	
	Porosity	Standard Deviation
Bottom Center	0.05	
Bottom Left	0.03	
Bottom Right	0.03	
CenterCenter	0.04	
Center Left	0.09	
Center Right	0.04	
Top Center	0.29	
Top Left	0.23	
Top Right	0.06	
TOTAL	0.86	0.0961914

c)

Figure 4.24. Inconel 718 samples a) 4 b) 5 c) 6 total porosity level.

Figure 4.24. above represents the total porosity level using chosen optimal scan speed and step over parameters on Inconel 718 samples a) 4 b) 5 c) 6.

Areas of Sample 7	Average Porosity Level [%]	
	Porosity	Standard Deviation
Bottom Center	0.1	
Bottom Left	0.13	
Bottom Right	0.06	
CenterCenter	0.06	
Center Left	0.18	
Center Right	0.09	
Top Center	0.14	
Top Left	0.14	
Top Right	0.22	
TOTAL	1.12	0.0534114

a)

Areas of Sample 8	Average Porosity Level [%]	
	Porosity	Standard Deviation
Bottom Center	0.08	
Bottom Left	0.14	
Bottom Right	0.04	
CenterCenter	0.12	
Center Left	0.19	
Center Right	0.09	
Top Center	0.06	
Top Left	0.09	
Top Right	0.12	
TOTAL	0.93	0.045

b)

Areas of Sample 9	Average Porosity Level [%]	
	Porosity	Standard Deviation
Bottom Center	0.04	
Bottom Left	0.04	
Bottom Right	0.07	
CenterCenter	0.3	
Center Left	0.06	
Center Right	0.05	
Top Center	0.08	
Top Left	0.13	
Top Right	0.14	
TOTAL	0.91	0.0829826

c)

Figure 4.25. Inconel 718 samples a) 4 b) 5 c) 6 total porosity level.

Figure 4.25. above represents the total porosity level using experimental genreated scan speed and step over parameters on Inconel 718 samples a) 7 b) 8 c) 9.

Table 4.2. Official EOS, optimal and experimental parameters of porosity level.

Sample	Average Porosity Level [%]		Average Pore Density Level [1/mm^2]	
	Porosity	Standard Deviation	Pore Density	Standard Deviation
1	0.66	0.04	30.91	2.22
2	1.24	0.08	73.32	6.69
3	1.14	0.08	65.74	5.68
4	0.65	0.03	29.45	1.97
5	1.46	0.11	88.79	7.09
6	0.86	0.09	47.23	5.30
7	1.12	0.05	52.75	2.80
8	0.93	0.04	46.8	2.80
9	0.91	0.08	51.89	4.67

Pore density levels and percentage of porosity levels of each sample (official EOS, chosen optimal and experimental parameters) along with the standard deviation are shown in the Table 4.3 above.

According to the data shown on Table 4.3, pore density values were compared among themselves in the Figure 4.28 below. At the same time, according to the data provided in the same table, percentage porosity values were compared among themselves in the Figure 4.29 and Figure 4.30 below. When the data was analysed (Figure 4.28, Figure 4.29 and Figure 4.30), percentage of porosity levels and pore density levels were adequate. According to those results, the percentage of porosity range is 0,65% to 1,46% (minimum to max) also standard deviation value is 0,03 to 0,11 respectively. The smallest porosity level was seen at sample 4 however the biggest porosity level was seen at sample 5 which is presents Figure 4.30 below. As shown in Table 4.3, Simple 4 (least porosity) and sample 5 (most porosity) were built based on chosen optimal parameters among themselves. Different porosity levels were observed on samples despite of the using the same parameters. However, sample 1 is shown 0,66%

porosity level. This result is highly close to the least porosity level (sample 4, porosity 0.65%). Additionally, the same parameters (official accepted EOS parameters) were applied for sample 1, sample 2 and sample 3 even so different porosity levels were observed on each three samples. Therefore, paired samples *t* test was applied for two different groups of parameters with the use of the IBM SPSS Statistics software. (official accepted EOS parameters: sample 1, 2, 3 and chosen optimal parameters: sample 4, 5, 6)

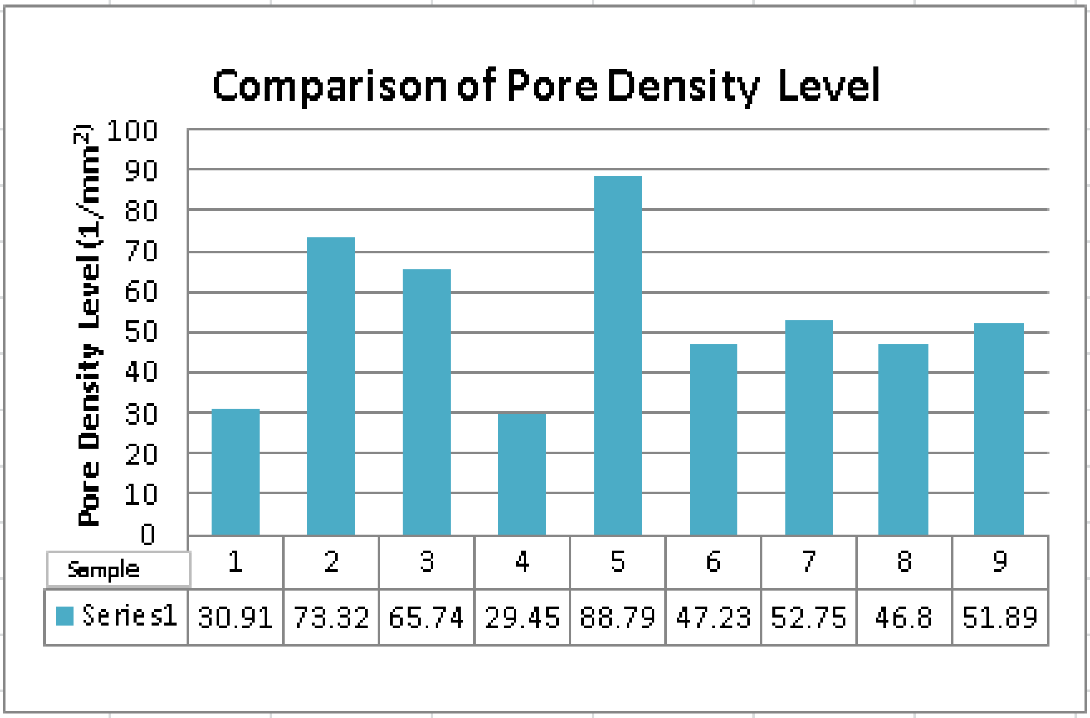

Figure 4.26. Comparison of pore density level.

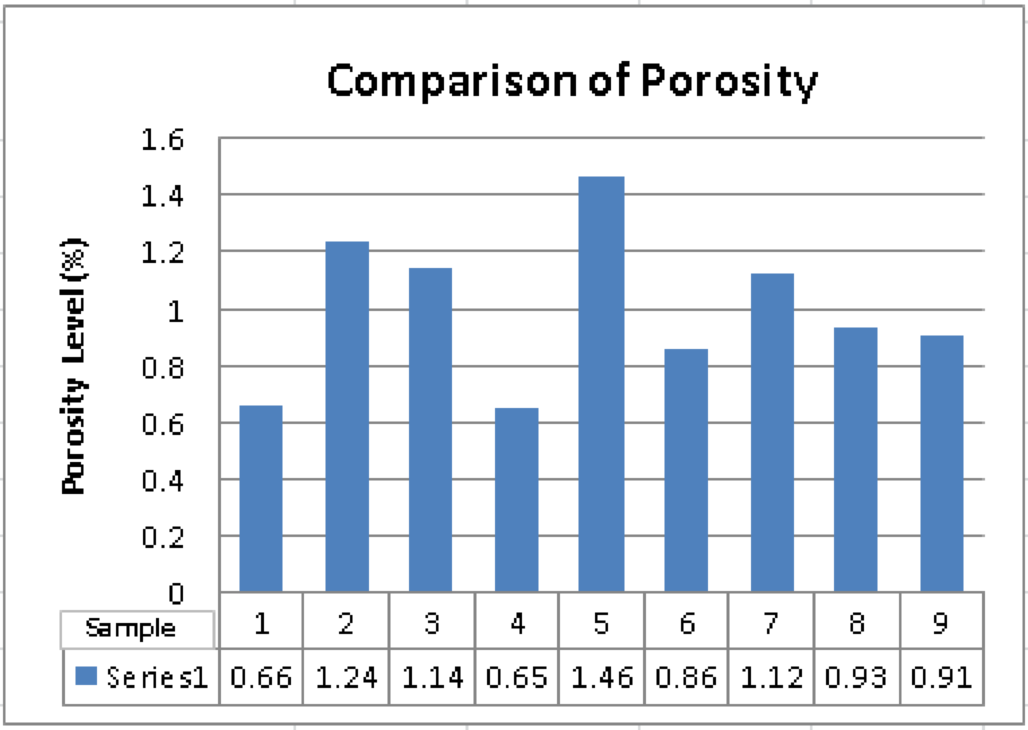

Figure 4.27. Comparison of porosity level.

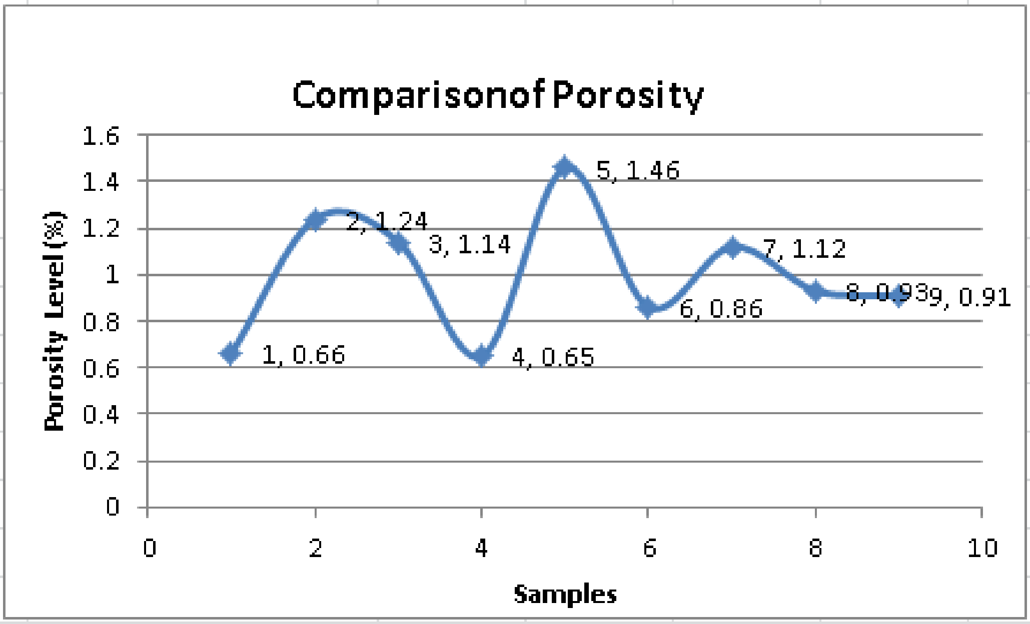

Figure 4.28. Comparison of porosity level.

Paired Samples Statistics

		Mean	N	Std. Devisation	Std. Error Mean
Pair 1	Sample1_2_3	1.0133	3	.31005	.17901
	Sample4_5_6	.9900	3	.42036	.24269

Paired Samples Correlations

		N	Correlations	Sig.
Pair 1	Sample1_2_3 & Sample4_5_6	3	.806	.403

Paired Samples Test

Pair 1	Mean	Std. Devisation	Std. Error Mean	95% Confidence Internal of the Difference
				Lower
Sample1_2_3 -Sample4_5_6	0.2333	.25027	.14449	.59836

Paired Samples Test

	Paired Differences	t	df	Sig. (2-tailed)
	95% Confidence Internal of the Difference			
	Upper			
Sample1_2_3 -Sample4_5_6	.64503	.161	2	.887

Figure 4.29. Paired *t* test results for porosity levels.

According to results of t test; sigma (p-value) is less than 0,05 (alpha) therefore there are difference values that comparison can be made between two groups. However, mean porosity value of sample 4, 5 and 6 is less than mean porosity value of sample 1, 2 and 3 (0,9900 < 1,0133) which is shown in the Figure 4.31 above. Based on these results, chosen optimal parameters (scan speed 1400 and step over distance 0.08) have shown less porosity level than official accepted parameters (scan speed 1200 and step over 0,09) with a difference of 0,02%.When analysed comparisons in the Figure 4.32 below, least porosity level is 0.91% (scan speed 1500 and step over distance 0.08). Additionally, the biggest porosity level is 1,12% (scan speed 1300 and step over distance 0,08).

In this case, sample 8 and Sample 9 that produced on the basis of experimental parameters were showed good surface quality in terms of percentage porosity level.

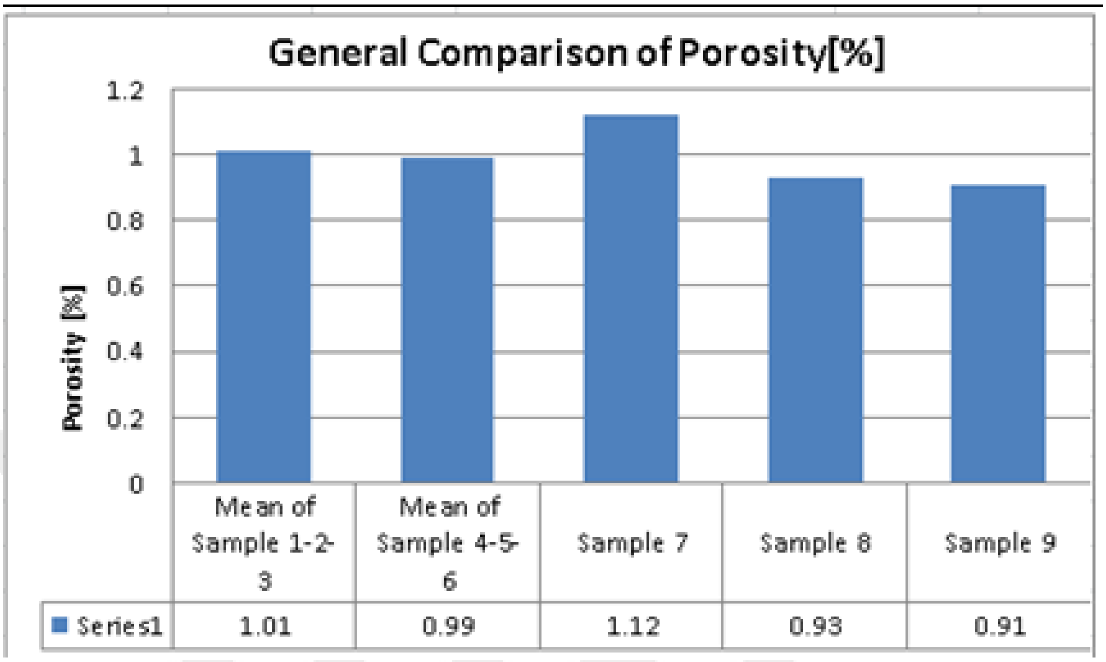

Figure 4.30. General comparison of porosity level.

Table 4.5. Effect of scan speed and time on porosity level.

Samples	Porosity(%)	Scan Speed	Step over	Power
Mean of Sample 4-5-6	0.99	1400		
Sample 7	1.12	1300	0.08	195
Sample 9	0.91	1500		

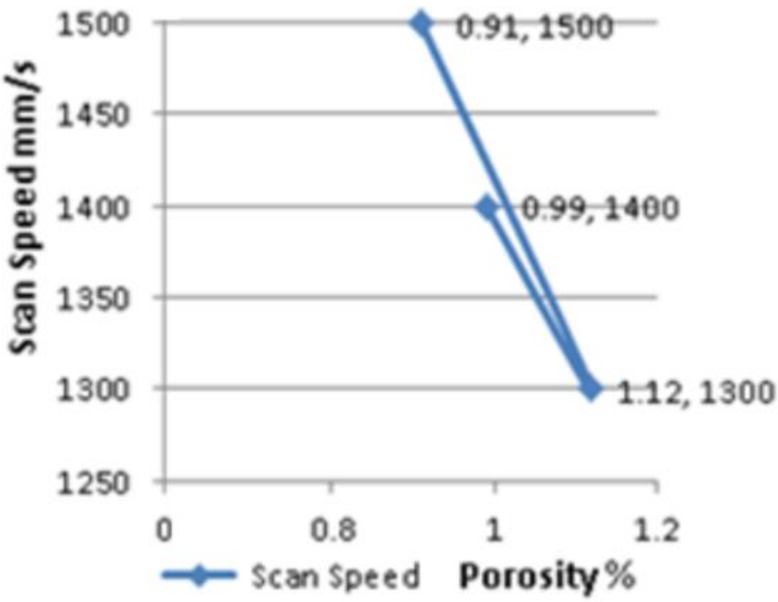

Figure 4.31. Effect of scan speed and time on porosity level [%].

According to data of Figure 4.33 and Figure 4.34 when scan speed is decreased (time increases), porosity level increases under the constant step over and laser power parameters. This information indicates that the time is directly proportional to porosity. However, this information was observed from only three different porosity values.

According to data of Figure 4.35 and Figure 4.36 below; when porosity level at lowest (0,1%), energy density is 1,7411(J/mm^2) and when porosity level at highest (6,99%), energy density is 2,7857 (J/mm^2). Thus, energy density and porosity values were observed to be in the direct proportion.

Table 4.6. Energy density and porosity.

Samples	Parameters			Energy Density	Average Porosity (%)	
	Scan Speed (mm/s)	Step over distance (mm)	Power (W)	(J/mm²)	Porosity	Standard Deviatio
1		0.05		2.7857	6.99	3.06
2		0.06		2.3214	0.28	0.001
3		0.07		1.9898	0.18	0.03
4		0.08		1.7411	0.1	0.41
5	1400	0.09		1.5476	1.23	0.31
6		0.1		1.3929	0.3	0.03
7		0.11		1.2662	1.42	0.18
8		0.12		1.1607	0.54	0.09
9		0.13		1.0714	0.54	0.05
1	1200	0.09	195	1.8055	0.66	0.04
2	1200	0.09		1.8055	1.24	0.08
3	1200	0.09		1.8055	1.14	0.08
4	1400	0.08		1.741	0.65	0.03
5	1400	0.08		1.741	1.46	0.11
6	1400	0.08		1.741	0.86	0.09
7	1300	0.08		1.875	1.12	0.05
8	1400	0.07		1.9897	0.93	0.04
9	1500	0.08		1.625	0.91	0.08

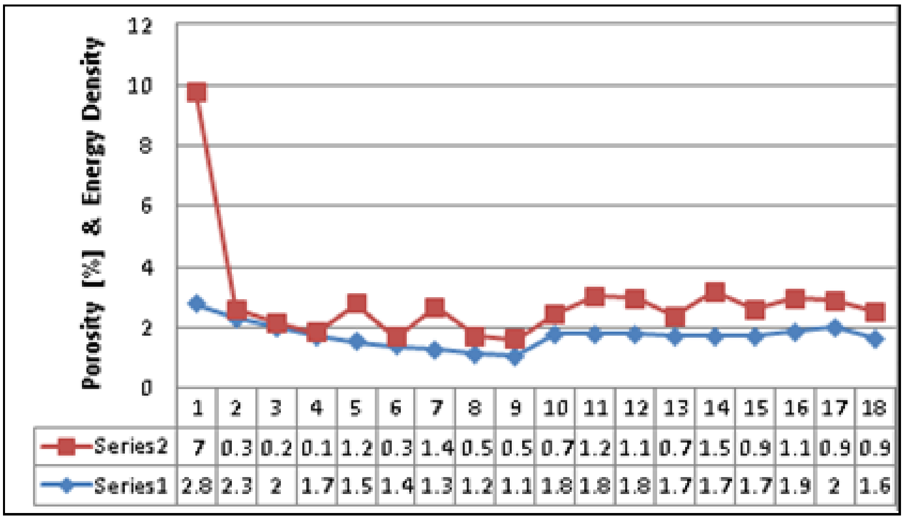

Figure 4.32. Energy density and porosity.

The results of tests and investigations are that decrease of the laser scan speed has remarkable effect on samples. Especially, roughness and irregularities were observed due to balling and spatter. Besides, increase of porosity level was observed with the deceasing levels of laser speed.

Similarly to the this study, most resarch stuties focused to improve laser sintering process such as parameters development [18- 20].

Eespecially, the material porwder characteristic such as particle size and particle shape also, the processig parameters such as laser power, scan speed and spot size factors were the key focus areas for those studies. However, very limited materials only for DMLS have been commercially available in spite of the various investigation of the metal powder systems [21]. On the other hand, insufficient powder melting can also result of high scan speeds parameters which invariably will result to lower relative densities continuously [92]. Most of studies have reported that the resolution of parts and surface roughness are mostly determined by the laser processing parameters [93]. Similiray to result of this study, Morgan et al. reported that higher scan speed and step over distance resulted to less amount of porosity and thus more intensive stainless steel samples after laser melting [83].

As well as effect of step over distance on the porosity level was observed on this study. However, effect of step over distance parameters on the porosity level is quite variable. Therefore, the drawing a linear graph to effect of step over distance parameters on the porosity level is difficult based on those results.

In addition to, it is noted that compared to the scan speed, the parameter of step over distance has a relatively lower effect on porosity and density of materials [83-94]. Additionally, Abele et al [79] explained that the effect of scan speed can be dependent to the overall energy density in the system.

At the same time, effect of scan speed was related to the energy density in this investigation which is shown Figure 4.35 and Figure 4.36 above. Energy density and porosity values were observed to be in the direct proportion

PART 5

SUMMARY

5.1. CONCLUSION AND RECOMMENDATION

The aim of this study was to ascertain optimal scan speed and step over distance parameters in the laser melting for Inconel 718 at the same time to document effect of step over and scan speed parameters on the quality of the samples. In accordance with the objectives, to achieve a quality result reference from the accepted parameters was taken; various scan speed and step over distance parameters 12 mm x 12 mm x 5 mm cross sectional INCONEL 718 samples were produced. The samples were used, examined and compared with respect to surface quality, balling, spatter and porosity. Tests were made in order to generate elements of the samples with different scan speed and step over parameters while keeping the laser power same at 195 W. Additionally, the produced samples were compared with new experimental parameters and official accepted EOS parameters. As a result of investigations, chosen optimal parameters (scan speed 1400 and step over distance 0,08) has shown smaller porosity level than the official accepted EOS parameters (scan speed 1200 and step over 0,09) with a difference of 0,02%. According to overall results, speed setting of 1400 mm/s, step over distance of 0.08 mm are recommended as optimum parameters for Inconel 718 on the EOS M270 laser melting machine. In addition to, (scan speed 1500 and step over distance 0.08) that was produced on the basis of experimental parameters showed good surface quality in terms of percentage porosity level. This result showed that the used experimental parameters (higher or equal than scan speed values of 1400mm) can be appropriate to achieve good results for next investigations.

Krishnan et al [104] studied the change in parameters of AlSi10Mg alloy using direct metal laser sintering similar to this study. Likewise, there was a significant change to the mechanical properties ogf the samples built. The parameters that were affected were the step over distance and the scan speed. In their study, the scanning speed was reduced from 900 to 700mm/s. Then the porosity was increased by reducing the laser power from 195W to 180W. These results indicated that decrease of the laser power should be avoided if the scan speed is desired to increase. Therefore, the outcome of this study fills the gap in the literature regarding the effect of laser power and laser scan speed paramets together on surface quality.

There are some limitations in this study as in each research. Foremost among these is the time and equipment. For instance, insufficient polishing process can affect to evaluation of porosity level. More samples should be produced and more tests made in order to achieve more effective results. This research is also limited according to the experimental approach of varying scan speed and step over distance parameters. In this study, only the effects of scan speed and step over parameters on porosity level were investigated.

5.2. FUTURE STUDY

In this study, the lower porosity level thus better surface quality was achieved by keeping laser power constant at 195W, using higher scan speed at 1400mm/sec as opposed to standard 1200mm/s, and using lower step over distance value at 0.08mm as opposed to standard 0,09mm. However, the effects of parameters on mechanical properties other than the surface quality was not investigated. Future studies could focus investigating these, such effects of alternative parameter settings on tensile, yield, breaking and impact strength. In this respect, alternative control parameters could be identified as per specific conditions and needs for EOS M270. Furthermore, improvements in adaption and the use range of EOS M270 built Inconel 718 alloys could be achieved.

REFERENCES

1. D. Atkinson, "Rapid Prototyping and Tooling, A Practical Guide", ***Strategy Publication Ltd, Welwyn Garden City,*** UK, (1997).

2. Gu D, Shen Y. "Influence of reinforcement weight fraction on microstructure and properties of submicron WC–Cop/Cu bulk MMCs prepared by direct laser sintering." ***J Alloys Compd*** 431:112–20, (2007).

3. Simchi A. "Direct laser sintering of metal powders: mechanism, kinetics and microstructural features." ***Mater Sci Eng A*** 428:148–58, (2006).

4. F. Klocke, T. Celiker, Y.A. Song, "Rapid metal tooling", ***Rapid Prototyping J.*** 1 (3),32–42, (1995).

5. G.B. Prabhu, D.L. Bourell, in: "Proceedings of the Solid Freeform Fabrication Symposium on Supersolidus Liquid Phase Selective Laser Sintering of Prealloyed Bronze Powder", ***The University of Texas at Austin***, pp. 317–324, (1993).

6. M. Greulich, H.D. Kunze, M. Greul, T. Pintat, "Laser Sintering of Metal Powders", ***Rapid Prototyping and Tooling Newsletter, No. 9, Danish Tech. Institute***, pp. 14–15, (1996)

7. H.J. Niu, I.T.H. Chang, "Selective laser sintering of gas and water atomized of high speed steel powders", ***Scripta Mater.*** 41 (1) 25–30, (1999).

8. H.J. Niu, I.T.H. Chang, "Liquid phase sintering of M3/2 high speed steel by selective laser sintering", ***Scripta Mater.*** 39 (1),67–72, (1998).

9. H.J. Niu, I.T.H. Chang, "Instability of scan tracks of selective laser sintering of high speed steel powder", ***Scripta Mater***. 41 (1) 1229–1234, (1999).

10. S. Das, T.P. Fuesting, G. Danyo, L.E. Brown, J.J. Beaman, D.L. Bourell, "Direct laser fabrication of superalloy cermet abrasive turbine blade tips", ***Mater. Des***. 21 63–73, (2000).

11. T. Laoui. L. Froyen, J.P. Kruth, in: "Proceedings of the PM World Congress on Effect of Mechanical Alloying on Selective Laser Sintering of WC–Co Hard Metal Powder", ***Granada*** , vol. 5, pp. 394–399, (1998).

12. C. Hauser, T.H.C. Childs, K.W. Dalgarno, R.B. Eane, "Atmospheric control during direct selective laser sintering of stainless steel", ***The University ofLeeds, UK*** 314S.

13. S. Das, J.J. Beaman, M. Wohlert, D.L. Bourell, "Direct laser freeform fabrication of high performance metal components", ***Rapid Prototyp. J. 4*** (3) 112–117, (1998).

14. O. Nyrhila, J. Kotila, J.-E. Lind, T. Syvanen, "Industrial use of direct metal laser sintering", in: ***Proceedings of the SFF, Austin,*** TX, August 10–12, (1998).

15. F. Petzoldt, M. Greul, H. Löffler, "Direct Metal Laser Sintering: Different Application/Different Material Concepts, Advances in Powder Metallurgy and Particular Materials", vol. 2, No. 5, MPIF, ***Princeton, NJ***, , pp. 71–76. (1999).

16. H. Pohl, "Direct Laser Sintering, EPMA Short Course on Sintering Science and Practice", ***Bremen,*** September (1999).

17. D.L. Bourell, H.L. Marcus, J.W. Barlow, J.J. Beaman, "Selective laser sintering of metals and ceramics", ***Int. J. Powder Metall.*** 28 (4), 369–381, (1992).

18. H.H. Zhu, L. Lu, J.Y.H. Fuh, "Influence of binder's liquid volume fraction on direct laser sintering of metallic powder", ***Mater. Sci. Eng.*** A 371 170–177, (2004).

19. A. Simchi, H. Pohl, "Direct laser sintering of iron-graphite powder mixture", ***Mater. Sci. Eng.*** A. 383,191–200,(2004).

20. A. Simchi, F. Petzoldt, H. Pohl, "On the development of direct metal laser sintering for rapid tooling, J. Mater. Process". ***Technol***. 141,319–328, (2003).

21. Y. Tang, H.T. Loh, Y.S. Wong, J.Y.H. Fuh, L. Lu, X. Wang, "Direct laser sintering of a copper-based alloy for creating three-dimensional metal parts", ***J. Mater. Process. Technol.*** 140, 368–372, (2003).

22. SHISHKOVSKY, I. "Synthesis of functional gradient parts via RP methods. Rapid Prototyping" Journal. Volume 7, issue 4, pages 207-211, DOI: ***http://dx.doi.org/10.1108/13552540110402908***, (2001).

23. TAY, B. Y.; EVANS, J. R. G.; EDIRISINGHE, M. J. "Solid freeform fabrication of ceramics." ***International Materials Reviews***, v. 48, n.6, p.341-370, (2003).

24. OLIVEIRA, M. F. "Aplicações da prototipagem rápida em projetos de pesquisa. Dissertação (Mestrado)" –***Universidade Estadual de Campinas, Campinas,*** (2008).

25. EFUND "Rapid Prototyping." Acessed on <***http://www.efunda.com/processes/rapid_prototyping/intro.cfm***>,(2014).

26. T.J. Horn, O.L.A. Harrysson "Overview of current additive manufacturing technologies and selected applications" ***Sci. Prog***. pp. 255–282, 95 (2012).

27. K.V. Wong, A. Hernandez "A review of additive manufacturing ISRN Mech." ***Eng***., pp. 1–10, (2012).

28. E. Louvis, P. Fox, C.J. Sutcliffe "Selective laser melting of Aluminium components." ***J. Mater. Process.Technol***., 211, pp. 275–284 (2011).

29. E. Brandl, U. Heckenberger, V. Holzinger, D. Buchbinder "Additive manufactured $AlSi_{10}Mg$ samples using Selective Laser Melting (SLM): microstructure, high cycle fatigue, and fracture behaviour Mater". ***Des.***, 34, pp. 159–169, (2012).

30. F. Wang, S. Williams, M. Rush "Morphology investigation on direct current pulsed gas tungsten arc welded additive layer manufactured Ti6Al4V alloy Int. J. Adv. Manuf." ***Technol***., 57, pp. 597–603 (2011).

31. Q. Jia, D. Gu "Selective laser melting additive manufacturing of Inconel 718 superalloy parts: densification, microstructure and properties." ***J. Alloys Compd***., 585, pp. 713–721(2014).

32. P. Kazanas, P. Deherkar, P. Almeida, H. Lockett, S. Williams "Fabrication of geometrical features using wire and arc additive manufacture." ***Proc. Inst. Mech. Eng. B: J. Eng. Manuf***., 226, pp. 1042–1051 (2012).

33. S. Rawal, J. Brantley, N. Karabudak "Additive manufacturing of Ti-6Al-4V alloy components for spacecraft applications." ***6th International Conference on Recent Advances in Space Technologies (RAST)***, IEEE, pp. 5–11 (2013).

34. B. Dutta, F.H.S. Froes "Additive manufacturing of titanium alloys" ***Adv. Mater. Process***., 172, pp. 18–23 (2014).

35. WOHLER T. "Wohlers report 2008." ***Fort Collins, Colorado***: Wohlers Associates (2008).

36. BUSATO, F. A. "Parâmetro de moldagem por injeção de termoplásticos em moldes fabricado por estereolitografia com resina Somos 7110. Universidade Federal de Santa Catarina, tese de mestrado." ***Florianópolis***. (2004).

37. EOS "Additive Manufacturing." Acessed on ***<http://www.eos.info/additive_manufacturing>,*** (2014).

38. M. Rombouts, J.P. Kruth, L. Froyen, P. Mercelis, "Fundamentals of selective laser melting of alloyed steel powders." ***CIRP Ann. Manuf. Technol***. 55 187–192, (2006).

39. J.P. Kruth, L. Froyen, J. Van Vaerenbergh, P. Mercelis, M. Rombouts, B. Lauwers, "Selective laser melting of iron-based powder." ***J. Mater. Process. Technol.*** 149 616–622, (2004).

40. X. Zhou, K. Li, D. Zhang, X. Liu, J. Ma, W. Liu, Z. Shen, "Textures formed in a CoCrMo alloy by selective laser melting." ***J. Alloy. Compd.*** 631, 153–164 (2015).

41. D. Gruner, Z. Shen, "Ordered coalescence of nano-crystals during rapid solidification of ceramic melts." ***CrystEngComm*** 13 5303–5305, (2011).

42. K. Saeidi, X. Gao, Y. Zhong, Z.J. Shen, "Hardened austenite steel with columnar sub-grain structure formed by laser melting." ***Mater. Sci. Eng. A-Struct***. 625 221–229, (2015).

43. S. Dadbakhsh, L. Hao, N. Sewell, "Effect of selective laser melting layout on the quality of stainless steel parts." ***Rapid Prototyping J***. 18 241–249 (2012).

44. H. Gong, Effect of Defects on Fatigue Tests of As-Built Ti-6Al-4V Parts Fabricated By "Selective Laser Melting, Solid Freeform Fabrication Symposium" ***the University of Texas at Austin***, ***Austin, U.S***., pp. 499–506 (2012).

45. D. Dai, D. Gu, "Tailoring surface quality through mass and momentum transfer modelling using a volume of fluid method in selective laser melting of TiC/AlSi10Mg powder." ***Int. J. Mach. Tools Manuf.*** 88 95–107,(2015).

46. E. Chlebus, B. Kuźnicka, R. Dziedzic, T. Kurzynowski, "Materials Science and Engineering" ***Mater. Sci. Eng. A*** 620 155–163 (2015).

47. H. Attar, L. Löber, A. Funk, M. Calin, L.C. Zhang, K.G. Prashanth, S. Scudino, Y.S. Zhang, J. Eckert,"Materials Science and Engineering" ***Mater. Sci. Eng.*** A 620,350–356, (2015).

48. P. Li, Z. Wang, N. Petrinic, C.R. Siviour, "Materials Science and Engineering" ***Mater. Sci. Eng.*** A 614,116–121, (2014).

49. P. Kanagarajah, F. Brenne, T. Niendorf, H.J. Maier, "Materials Science and Engineering" ***Mater. Sci. Eng.*** A 588,188–195,(2013).

50. X.P. Li, C.W. Kang, H. Huang, L.C. Zhang, T.B. Sercombe, "Materials Science and Engineering" ***Mater. Sci. Eng.*** A 606,370–379, (2014).

51. B. Song, S.J. Dong, C. Coddet, "Review of selective laser melting: Materials and applications" ***Scr. Mater.*** 75,90–93, (2014).

52. D.E. Cooper, N. Blundell, S. Maggs, G.J. Gibbons, J. Mater. "Additive layer manufacture of Inconel 625 metal matrix composites, reinforcement material evaluation" ***Technol***. 213 2191–2200, (2013).

53. H.P. Tang, G.Y. Yang, W.P. Jia, W.W. He, S.L. Lu, M. Qian, "Materials Science and Engineering" ***Mater. Sci. Eng.*** A 636, 103–107, (2015).

54. N.J. Harrison, I. Todd, K. Mumtaz, "Reduction of micro-cracking in nickel superalloys processed by Selective Laser Melting: A fundamental alloy design approach" ***Acta Mater***. 94,59–68,(2015).

55. H. Attar, M. Bönisch, M. Calin, L.C. Zhang, S. Scudino, J. Eckert," Additive Manufacturing Processes: Selective Laser Melting, Electron Beam Melting and Binder Jetting—Selection Guidelines" ***Acta Mater.*** 76, 13–22, (2014).

56. S. Das, "Physical Aspects of Process Control in Selective Laser Sintering of Metals" ***Adv. Eng. Mater***. 5, 701–711, (2003).

57. L.C. Zhang, D. Klemm, J. Eckert, Y.L. Hao, T.B. Sercombe, "Manufacture by selective laser melting and mechanical behavior of a biomedical Ti–24Nb–4Zr–8Sn alloy", ***Scr. Mater***. 65,21–24, (2011).

58. R. Li, Y. Shi, Z. Wang, L. Wang, J. Liu, W. Jiang, "Densification behavior of gas and water atomized 316 L stainless steel powder during selective laser melting", ***Appl. Surf. Sci.*** 256 (13) ,4350–4356,(2010).

59. K.G. Prashanth, H. Shakur Shahabi, H. Attar, V.C. Srivastava, N. Ellendt, V. Uhlenwinkel, J. Eckert, S. Scudino, "Production of high strength Al 85 Nd 8 Ni 5 Co 2 alloy by selective laser melting", ***Addit. Manuf. 6 ,*** 1–5 (2015).

60. K.G. Prashanth, S. Scudino, H. Klauss, K.B. Surreddi, L. Löber, Z. Wang, A.K. Chaubey, U. Kühn, J. Eckert, "Microstructure and mechanical properties of Al–12Si produced by selective laser melting: effect of heat treatment", ***Mater. Sci. Eng.*** A 590,153–160, (2014).

61. T. Vilaro, C. Colin, J.D. Bartout, "A Review of the As-Built SLM Ti-6Al-4V Mechanical Properties towards Achieving Fatigue Resistant Designs", ***Metall. Mater. Trans.*** A 42, 3190–3199, (2011).

62. C.L. Qiu, N.J.E. Adkins, M.M. Attallah, "Microstructure and tensile properties of selectively laser-melted and of HIPed laser-melted Ti–6Al–4V", ***Mater. Sci. Eng.*** A 578,230–239, (2013).

63. C.L. Qiu, S. Yue, N.J.E. Adkins, M. Ward, H. Hassanin, P.D. Lee, P.J. Withers, M.M. Attallah, "Influence of processing conditions on strut structure and compressive properties of cellular lattice structures fabricated by selective laser melting", ***Mater. Sci. Eng.*** A 628, 188–197, (2015).

64. C. Panwisawas, C.L. Qiu, Y. Sovani, J.W. Brooks, M.M. Attallah, H.C. Basoalto, "On the role of thermal fluid dynamics into the morphological development of porosity during selective laser melting", ***Scr. Mater.*** 105 ,14–17, (2015).

65. L. Thijs, F. Verhaeghe, T. Craeghs, J. Van Humbeeck, Jean-Pierre Kruth, A study of the microstructural evolution during selective laser melting of Ti–6Al–4V, Acta Mater. 58 (2010) 3303–3312.

66. W. Xu, M. Brandt, S. Sun, J. Elambasseril, Q. Liu, K. Latham, K. Xia, M. Qian, Additive manufacturing of strong and ductile Ti–6Al–4V by selective laser melting via in situ martensite decomposition, Acta Mater. 85 (2015) 74–84.

67. M.M. Ma, Z.M. Wang, M. Gao, X.Y. Zeng, "Layer thickness dependence of performance in high-power selective laser melting of 1Cr18Ni9Ti stainless steel", ***J. Mater. Process. Technol.*** 215,142–150,(2015).

68. Dewidar MM, Dalgarno KW, Wright CS. "Processing conditions and mechanical properties of high-speed steel parts fabricated using direct selective laser sintering." ***Proc Inst Mech Eng Part B: J Eng Manuf***. 217:1651–62, (2003).

69. Louvis E, Fox P, Sutcliffe CJ. "Selective laser melting of aluminium com-ponents." ***J Mater Process Technol*** ;211:275–84, (2003).

70. Kempen K, Thijs L, Yasa E, Badrossamay M, Verheecke W, Kruth J-P.Process "Optimization and microstructural analysis for selective laser melt-ing of AlSi10Mg; 2011." Available at: ***http://utwired.engr.utexas.edu/lff/symposium/proceedingsArchive/pubs/Manuscripts/2011/2011-37-Kempen.pdf [accessed May 2014].***

71. Olakanmi EO. "Selective laser sintering/melting (SLS/SLM) of pure Al,Al–Mg, and Al–Si powders: effect of processing conditions and powderproperties." ***J Mater Process Technol***, 213:1387–405, (2013).

72. Thijs L, Kempen K, Kruth J-P, Van Humbeeck J. "Fine-structured aluminiumproducts with controllable texture by selective laser melting of pre-alloyedAlSi10Mg powder." ***Acta Mater***; 61:1809–19 (2013).

73. Gusarov, A.V., Smurov, I., "Two-dimensional numerical modelling of radiation transfer in powder beds at selective laser melting." ***Appl. Surf. Sci.*** 255 (10), 5595–5599, (2009).

74. Gusarov, A.V., Smurov, I., "Modelling the interaction of laser radiation with powder bed at selective laser melting." ***Phys. Procedia 5 (Part B)***, 381–394 (2009).

75. Gusarov, A.V., Yadroitsev, I., Bertrand, Ph., Smurov, I. " Model of radiation and heat transfer in laser–powder interaction zone at selective laser melting." ***J. Heat Transfer*** 131 (7), (2009).

76. Dewidar MM, Dalgarno KW, Wright CS. "Processing conditions and mechanical properties of high-speed steel parts fabricated using direct selective laser sintering." Pr***oc Inst Mech Eng Part B: J Eng Manuf***; 217:1651–62 (2003).

77. Khan M, Dickens P. "Selective laser melting (SLM) of gold (Au).2 ***Rapid Prototyp J***. 18:81–94 (2012).

78. Read N, Wang W, Essa K, Attallah MA. "Selective laser melting of AlSi10Mg alloy: process optimisation and mechanical properties development." ***Mater Des***;65:417–24 (2015).

79. Abele, E., Stoffregen, H. A., Kniepkamp, M., Lang, S., Hampe, M." Selective laser melting for manufacturing of thin-walled porous elements", ***Journal of Materials Processing Technology,*** Vol. 215, pp. 114-122 (2012).

80. Zheng, L., Liu, Y., Sun, S., Zhang, H. " Selective laser melting of Al–8.5Fe–1.3V–1.7Si alloy: Investigation on the resultant microstructure and hardness", ***Chinese Journal of Aeronautics,*** Vol. 28, Issue 2, pp. 564-569, (2015).

81. Xie, J.W., Fox, P., O'Neill, W., Sutcliffe, C.J." Effect of direct laser re-melting processing parameters and scanning strategies on the densification of tool steels", ***Journal of Materials Processing Technology***, Vol. 170, Issue 3, pp. 516-523 (2005).

82. Khan, M., Dickens, P. "Selective laser melting (SLM) of gold (Au)", ***Rapid Prototyping Journal,*** Vol. 18 Iss: 1, pp.81 – 94 (2012).

83. Morgan, R., Sutcliffe, C.J., O'Neill, W. "Density analysis of direct metal laser re-melted 316L stainless steel cubic primitives", ***Journal of Materials Science,*** 39 (4), pp. 1195–1205, (2004).

84. Gibson, I., Dongping, S. "Material properties and fabrication parameters in selective laser sintering process." ***Rapid Protyping Journal***. Vol. 3, No. 4. MCB University Press. p. 129-136, (1997).

85. Hens KF, Grohowski JA, German RM, Valencia JJ, McCabe T." Processing of Superalloys via Powder Injection Molding, Advances in PM and Particulate Materials", ***MPIF, 4***;. p. 137–48, (1994).

86. Nickel Based "Alloys and methods of heat treating nickelbased alloys", ***US Patent No***: 7156932 (1999).

87. John P. Collier, Song How Wong, John K. Tien and James C. Phillips, "The effect of varying AI, Ti and Nb content on the phase stability of INCONEL 718", ***Metallurgical and Materials Transactions A***, Volume 19, Number 7/July, (1988).

88. R.E. Schafrik, D.D. Ward, J.R. Groh, in: E.A. Loria (Ed.), "Proceedings of the Fifth International Symposium on Superalloys 718, 625, 706 and Various Derivatives", ***TMS, Warrendale, PA,*** pp. 1–12 (2012).

89. R.P. Jewett, J.A. Halchak, in: E.A. Loria (Ed.), "Proceedings of the Second International Symposium on Superalloys 718, 625, and Various Derivatives", ***TMS, Warrendale, PA,*** pp. 749–760 (1991).

90. A.R. Brown, J.F. Radavich, P. Stinner, in: E.A. Loria (Ed.)," Proceedings of the First International Symposium on Superalloys 718—Metallurgy and Applications", ***TMS, Warrendale, PA***, pp. 623–629 (1989).

91. H.F. Merrick, "Phase Transformations in High-Temperature Alloys of the Ni – Cr – Fe – Nb System" ***Met. Trans.*** A 7A (4) 505–514 (1976).

92. Louvis, E., Fox, P., Sutcliffe, C. J. "Selective laser melting of aluminium components, Journal of Materials Processing Technology" ***Vol.211***, ***Issue 2***, pp. 275-284 (2011).

93. Mumtaz, K. A, Hopkinson, N. "Selective laser melting of thin wall parts using pulse shaping, Journal of Materials Processing Technology", ***Vol. 210, Issue 2***, pp. 279-287 (2010).

94. Xie, J.W., Fox, P., O'Neill, W., Sutcliffe, C.J."Effect of direct laser re-melting processing parameters and scanning strategies on the densification of tool steels", ***Journal of Materials Processing Technology, Vol. 170, Issue 3***, pp. 516-523 (2005).

95. R. Noorani," Rapid Prototyping—Principles and Applications", ***John Wiley & Sons***,(2006).

96. Kruth, "A Review of Additive Manufacturing" ***Wong and Aldo***, p.3 (2012)

97. Silva, R. J. et al." 3D Metal Printing Technology" ***IFAC-Papers On Line*** 48-3 2318–2322 (2015).

98. Y. Liu et al. "Vaccine development and manufacturing" ***Materials and Design*** 87 797–806: p.798 (2015).

99. Senthikumaran et al. " Edge Detection Techniques for Image Segmentation A Survey of Soft ComputingApproaches" ***Bharathiar University India*** p. 2948 (2009).

100. ***Adapted from, EOS,*** "Material data sheet, EOS NickelAlloy IN718, TMS, WEIL " p.3 (2014)

101. ***Adapted from, EOS,*** "Material data sheet, EOS NickelAlloy IN718, TMS, WEIL" p.2 (2014).

102. ***Adapted from, EOS***, "Material data sheet, EOS NickelAlloy IN718, TMS, WEIL" p.4 (2014)

103. Adapted from, ***EOS Dental Brochure*** ,"Status 03/09 Technical data subject to change without notice. EOS®, EOSINT®, DMLS® and e-Manufacturing™ are registered trademarks of EOS GmbH. EOS is certified according to ISO 9001" p.8 (2014).

104. Krishnan M. et al. "On the effect of process parameters on properties of AlSi10Mg parts produced by DMLS", ***The international journal for research on additive manufacturing and 3D printing***, accepted 23rd November 2013, p.445-446 (2013).

APPENDIX

ERASMUS EXHANGE PROGRAMME CERTIFICATES

UNIVERSITY OF WOLVERHAMPTON

RETURN AT END OF PLACEMENT TO

Gill Fletcher
Student Support Officer
Student Centre
University of Wolverhampton
MX Ground Floor
Camp Street
Wolverhampton
WV1 1AD
UK Code: (01902) International Code (+44 1902)
Direct Line: 01902 322426
E-mail: gillfletcher@wlv.ac.uk

ERASMUS+
Certificate of STAY

I the undersigned B. Chodda

Function Student Advisor

Establishment (host University) University of Wolverhampton

Certify that (name of student) Abdullah Seyir

Commenced Exchange **On** 28/09/14

Completed Exchange **On** 30/09/15

Date 03/11/15

Signature B.Chodda.

Seal of the establishment

City Campus Molineux
MX Student Office
- 3 NOV 2015
UNIVERSITY OF WOLVERHAMPTON

Name of Student	Abdullah Seyir	Date of Birth	26/May/1989
University Reference	1422650/1	HESA Reference	1410854226506
Qualification Aim	University Statement of Credit	FHEQ Level	Undergraduate Credit

Teaching Institution	University Campus
Awarding Institution	University of Wolverhampton
Languages of Instruction	English
Programme of Study	UGCREDIT20
Route of Study	Erasmus Exchange Programme (Part Year)

Record of Learning and Achievement

2014/5	Level	Mark/ Grade	Credit
7ET023 Dissertation	7N	70%	60

Total credits gained 60

Date Transcript Issued: 2 November 2015

To check the validity of this transcript contact Student Records Unit, University of Wolverhampton, MX Building, Camp Street, Wolverhampton WV1 1AD, UK, fax no:+44 (0)1902-321896, and quote transcript number 1422650/12112015.

UNIVERSITY OF WOLVERHAMPTON

INTERNATIONAL CENTRE

RESUME

Abdullah Seyir was born in 1989 in Bursa, Turkey. He started secondary school education in 2004 and attended Ali Osman Sonmez ATL. After finishing 4 years of secondary school education he pursued higher education studies in Design and Machine Building Education at the University of Karabuk. He successfully graduated with a BSc Hons in 2013. He continued his higher education studies at the University of Karabuk and started his MSc in Industrial Design Engineering at the University of Karabuk. In 2014, he decided to embark on an Erasmus programme at the University of Wolverhampton and continued his thesis project there. Abdullah completed his thesis project with distinction awarded by the University of Wolverhampton in the same year. Soon after that he established his own business called Seyir Design and Training Ltd based in Wolverhampton, UK. He is currently providing mechanical design engineering and training services for companies especially in the West Midlands area, UK.

CONTACT INFORMATION

Address: Karabük University
Graduate School of Natural & Applied Science
Demir-Çelik Campus/KARABUK

E-mail: abdullahseyir@gmail.com & abdullah@seyirdesign.co.uk